Beneath the trees: the influence of natural capital on shadow price dynamics in a macroeconomic model with uncertainty

Ghassane Benmir, Aditya Mori, Josselin Roman
and Romano Tarsia

February 2025

The Grantham Research Institute on Climate Change and the Environment was established by the London School of Economics and Political Science in 2008 to bring together international expertise on economics, finance, geography, the environment, international development and political economy to create a world-leading centre for policy-relevant research and training. The Institute is funded by the Grantham Foundation for the Protection of the Environment and a number of other sources. It has five broad research areas:

1. Climate change impacts and resilience
2. Cutting emissions
3. Financing a better future
4. Global action
5. Protecting the environment

More information about the Grantham Research Institute is available at: www.lse.ac.uk/GranthamInstitute

Beneath the Trees: The Influence of Natural Capital on Shadow Price Dynamics in a Macroeconomic Model with Uncertainty*

Ghassane Benmir[1,2,3]   Aditya Mori[3]   Josselin Roman[4]   Romano Tarsia[2]

4 February 2025

Abstract

We investigate the impact of incorporating natural capital dynamics on optimal allocation in an economy subject to uncertainty. We present new estimates on climate damages to natural capital and elasticities of substitution between natural capital and other production inputs. Using these estimates, we examine how shadow prices vary across model specifications and parameter calibrations. Our findings indicate that the social cost of carbon is 12 percent higher in a model incorporating natural capital compared to a standard DICE-type model. Furthermore, the social cost of carbon is highly sensitive to the elasticity of substitution in the final output production function. Accounting for the stochastic nature of productivity further increases the social cost of carbon by 0.13 percent to 39 percent, depending on the inclusion of habit formation.

Keywords: Natural Capital, Shadow Prices, Social Cost of Carbon, Uncertainty.

JEL: *E6, Q2, Q5*

[1]IE University and Business School, P. de la Castellana, 259, Madrid; E-mail: ghassane.benmir@ie.edu.
[2]London School of Economics and Political Science, Houghton Street, London WC2A 2AE
[3]King's Business School and Qatar Centre for Global Banking & Finance, Strand, London WC2B 4BG
[4]European Commission – Joint Research Centre: josselin.roman@ec.europa.eu

1 Introduction

In this paper, we build a dynamic stochastic macroeconomic model featuring various types of natural capital and an emission externality to study the impact of including ecosystems dynamics in an otherwise standard macro-environment model. We present new estimates on climate damages to natural capital and elasticities of substitution between natural capital and other production inputs. Using these estimates, we examine how shadow prices vary across model specifications and parameter calibrations. We compare our model with natural capital to a standard DICE-type model. Our findings indicate that the social cost of carbon (SCC) is about 12 percent higher in the full model compared to the standard DICE-type model. Furthermore, we demonstrate that all shadow prices are highly sensitive to the elasticity of substitution in the final output production function, compared to the calibration of damage functions, climate dynamics, and discount rates noted in previous literature. Additionally, we compute the mean of the shadow prices, conditional on the expectation of shocks on productivity and temperature. We find that accounting for the stochastic nature of productivity further increases the SCC by 0.13 percent to 39 percent, depending on the inclusion of habit formation. Finally, we demonstrate that increased investments in renewables contribute to reducing the SCC over the long run.

Natural capital, encompassing natural resources like forests, minerals, water, and biodiversity, is crucial for economic production and human well-being. It provides essential ecosystem services, including clean air and water, soil fertility, and climate regulation, which underpin all economic activities. In turn, economic activity impacts ecosystems sustainability through rising temperature. Elevated temperatures intensify evapotranspiration and moisture stress in forests, degrade arable land conditions, increase cooling costs and reduce efficiency in mining operations, and decrease the efficiency of fossil fuel extraction and processing. These climatic impacts exacerbate vulnerabilities in forest ecosystems, cropland, mineral resources, and fossil fuels, leading to higher operational costs, reduced output, and instability in energy supplies. Despite its importance, natural capital is often overlooked in the macroeconomic literature, which traditionally focuses on manufactured capital and human capital. This omission leads to an incomplete understanding of economic systems and underestimates the long-term benefits of incorporating natural capital into economic analysis and policy-making.

Our paper makes two main contributions. First, on the empirical front, we estimate damage functions linking temperature changes to the stock of natural capital as well as elasticities of substitution between various types of natural capital entering the production process. Second, we use a macroeconomic model

to derive the shadow prices of these natural capital assets, highlighting the critical role of accounting for uncertainties around temperature fluctuations and Total Factor Productivity (TFP) variations. These contributions provide a deeper understanding of the economic value of natural capital and underscore the necessity of integrating it into economic models for sustainable development.

Given the scope of our paper, we contribute to three distinct strands of literature. The first, climate econometrics, seeks to understand the causal effects of climate on various socioeconomic variables such as mortality (Deschênes and Greenstone, 2011; Barreca, 2012; Carleton, Jina, Delgado, Greenstone, Houser, Hsiang, Hultgren, Kopp, McCusker, Nath, et al., 2022), agricultural output (Deschênes and Greenstone, 2007; Schlenker and Roberts, 2009; Burke and Emerick, 2016), industrial output (Graff Zivin and Kahn, 2016), labor productivity (Graff Zivin and Neidell, 2014; Somanathan, Somanathan, Sudarshan, and Tewari, 2021), and economic growth (Nordhaus, 2006; Dell, Jones, and Olken, 2012; Burke, Hsiang, and Miguel, 2015; Kotz, Levermann, and Wenz, 2024). Our paper focuses on the costs of climate change on natural capital. A closely related work by Bastien-Olvera, Conte, Dong, Briceno, Batker, Emmerling, Tavoni, Granella, and Moore (2024) estimates how climate change-induced changes in terrestrial vegetation cover impact economic production and the value of non-market ecosystem benefits. This paper bridges these two literatures by using climate econometrics methods to estimate the effect of higher temperatures on natural capital stocks. More specifically, we provide novel estimates of the economic costs of climate change resulting from damages to a broad set of natural capital variables, including cropland, forest ecosystem, minerals, coal, gas, oil, fossil fuel, and renewable energy.

Additionally, we contribute to the literature on the estimation of Constant Elasticity of Substitution (CES) functions. While Acemoglu, Aghion, Bursztyn, and Hemous (2012) and recent works such as Papageorgiou, Saam, and Schulte (2017) and Jo and Miftakhova (2024) have theorised and provided estimates respectively of CES parameters for production functions that aggregate dirty and clean energy inputs, our modeling framework is more disaggregated and requires estimating elasticities between various types of natural capital. We also utilize various estimation techniques to evaluate the robustness of our results in relation to the findings of Papageorgiou et al. (2017).

Finally, we contribute to the burgeoning literature on natural capital in macroeconomic models. The inclusion of climate dynamics in macroeconomic models can be traced back to Nordhaus (1991), which paved the way for a wide range of models known as Integrated Assessment Models (IAMs). However, this literature primarily focuses on the carbon cycle and the impact of rising temperatures on optimal economic allocation, without explicitly modeling natural capital. Recent works, such as Bastien-Olvera and Moore

(2021), Bastien-Olvera et al. (2024), and Drupp, Hänsel, Fenichel, Freeman, Gollier, Groom, Heal, Howard, Millner, Moore, et al. (2024), have started integrating the evolution of natural capital stock into their analyses.[1] Our modeling approach differs in two key ways. First, we do not fix the substitutability between input factors to unity (*i.e.* we do not assume Cobb-Douglas production functions) but instead estimate these parameters empirically. Second, we consider not only optimal allocation under deterministic scenarios but also assess the impact of the stochastic nature of temperature and productivity on various shadow prices.

To examine the impact of incorporating natural capital into optimal economic allocation, we develop a dynamic stochastic general equilibrium model (figure 1). In this model, output is generated from traditional production factors (produced and human capital) as well as renewable and non-renewable ecosystem assets (cropland, energy, minerals, and forests ecosystem services). Energy generation is divided between renewable and fossil sources. Crucially, the use of fossil fuels for energy production results in an externality: increased carbon concentrations in the atmosphere lead to rising temperatures. Sector-specific damage functions then link climate change to a reduction in output across different parts of the economy. A significant portion of the paper focuses on estimating these input-specific damage functions.
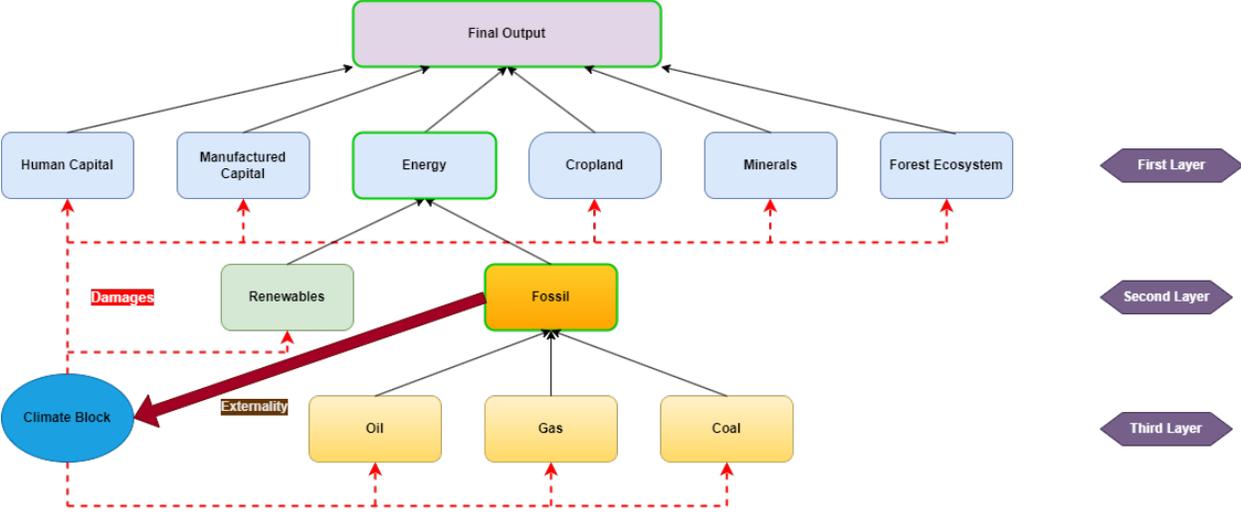
Figure 1: Structure of the Model

Another key feature of the model is the use of CES functions to aggregate production factors. While the use of the Cobb-Douglas production function is common in the literature, the CES specification is more general and provides insights into the substitutability of various production factors. Specifically, we assume that at each node where multiple inputs combine (materialized in the figure with a green edge), the elasticity

---

[1]Similarly, Drupp and Hänsel (2021), and Sterner and Persson (2008) introduce natural capital/ecosystem services into the utility function. We instead will incorporate biodiversity within the production function.

of substitution can range from zero (perfect complements) to infinity (perfect substitutes). Estimating these parameters is another important contribution of this paper. As demonstrated in our simulations, the values of these elasticities significantly impact the shadow prices of the production factors.

This paper is organized as follows: section 2 covers the data used and the estimation of CES and damage function parameters, section 3 outlines the macroeconomic model, section 4 discusses the results, and section 5 concludes.

2 Empirical Estimation

2.1 Data

The data utilized in this paper are categorized into two types: those employed for CES estimation and those used for estimating climate damages.

2.1.1 CES Estimation Data

For the CES estimation, we use the Changing Wealth of Nations (CWON) dataset, GDP data from the World Bank, and the Energy dataset from Our World In Data (OWID). The CWON provides a comprehensive account of produced, natural, and human capital for approximately 200 countries from 1995 to 2018. The OWID Energy dataset is a collection of energy metrics, which includes data on the consumption and production of various energy sources.

The data challenges in estimating CES production functions are twofold. First, the data must be in consistent units to ensure that parameter estimates are interpretable and unbiased. Second, the output variable data series cannot be a simple linear sum of the input variables. This is because using such data could result in biased parameter estimates by enforcing a non-linear fit where only a linear relationship exists.

To address the first challenge, the CWON dataset is used to estimate only the first layer with produced, natural, and human capital as inputs, while the output is derived from GDP data, with all variables measured in constant 2018 USD using country-specific GDP deflators. The CWON dataset also includes data on energy, which is an unweighted linear sum[2] of coal, gas, and oil, preventing its use for estimating the third layer as discussed above. Therefore, to address the second challenge we use the OWID Energy dataset, which provides production and consumption data in tera- or kilowatt-hours. Specifically, for the second

---

[2]Energy = Coal + Gas + Oil

layer, we use electricity demand as the output, with inputs being electricity generation from fossil fuels and renewable sources. For the third layer, we use electricity generation from fossil fuels as the output to maintain consistency with the second layer, while the inputs are coal, oil, and gas production.

Lastly, our inputs are stock variables and the output is GDP, which is a flow variable. A simplified version of our CES specification below features share parameter θ, substitution parameter ρ, scaling parameter $\tilde{g_Y}$ and produced and human capital as inputs. The latter is a stock because the data used defines it as the present value of all future earnings of the working population. Traditionally, a multiplicative term in the CES captures total factor productivity. However, in our case it can act as a more general scaling factor that also reflects the contribution of stock input variables to the flow output variable. To see how, note that a stock variable can be converted to a flow by multiplying the inputs by some discount rate r[3]. This discount rate can be factored out and we can restate the new multiplicative term as $g_Y = \tilde{g_Y} r$, which helps reconcile the stock-flow mismatch.

$$Y_{i,t} = \tilde{g_Y} \left(\theta (r Y_{i,t}^K)^{-\rho} + (1 - \theta)(r Y_{i,t}^{AL})^{-\rho} \right)^{\frac{-1}{\rho}} \tag{1}$$

Table 1 summarizes the variables used and their sources, while table 11 provides descriptive statistics of these variables. We exclude certain CWON natural capitals from the estimation procedure, such as mangroves, fisheries, and protected areas, due to questions regarding their relevance to the production of a representative world economy. For example, mangroves are rare across countries, making their inclusion inappropriate for a representative economy. Additionally, we do not include forest timber, as its inclusion in the CES results in an estimated production share of zero.

---

[3]The CWON dataset expresses all variables as discounted stock values, using a consistent discount rate for all variables.

Category	Symbol	Description	Unit	Source
First Layer Variables				
GDP	Y^T	GDP at purchaser's prices	2018 USD	World Bank
Capital	Y^K	Value of buildings and equipment	2018 USD	CWON
Human Capital	Y^{AL}	PV of future earnings for the population	2018 USD	CWON
Ecosystem	Y^{FO}	Forest ecosystem services	2018 USD	CWON
Cropland	Y^L	Agricultural Land	2018 USD	CWON
Minerals	Y^M	Composite of different minerals	2018 USD	CWON
Fossil Energy	Y^E	Oil, gas, hard and soft coal	2018 USD	CWON
Second Layer Variables				
Electricity Demand	Y^E	Demand for electricity	Terawatt Hours	OWID
Fossil Fuel Electricity	Y^{FE}	Electricity generation from fossil fuels	Terawatt hours	OWID
Renewable Electricity	Y^{RE}	Electricity generation from renewables	Terawatt hours	OWID
Third Layer Variables				
Oil-Gas Production	Y^G	Sum of gas and oil production	Terawatt hours	OWID
Coal Production	Y^C	Coal production	Terawatt hours	OWID

Table 1: Variable Summaries: CES Estimates Data

2.1.2 Natural Capital Climate Damages Estimation Data

In this paper, the types of natural capital considered include cropland, forest ecosystem services, minerals, and energy. Energy is further broken down as described earlier. While we use the CWON dataset for natural capital classification, their data reflect the market values of these resources, which might conflate the impact of temperature on the quantity of natural capital with its market value. To avoid this confusion, whenever possible, we used available data on the actual quantities of natural capital instead of their market valuations. For cropland, we used the Arable Land data from the World Bank, measured in hectares per capita, which we converted into hectares using population data. To obtain data on aggregate energy and its decomposition, we referred to the OWID Energy dataset as previously discussed. However, since quantity data were not available for forest ecosystem services and minerals,[4] we relied on the CWON dataset for these components. Lastly, we used temperature and precipitation data from the Climate Change Knowledge Portal. Table 2 summarizes the variables used and their sources, while table 12 provides summary statistics.

---

[4]Minerals in the CWON dataset include bauxite, copper, gold, iron ore, lead, nickel, phosphate, silver, tin, and zinc.

Description	Unit		Source
Total Cropland	Arable land	Hectares	World Bank
Coal Electricity	Electricity generation from coal	Terawatt hours	OWID
Gas Electricity	Electricity generation from gas	Terawatt hours	OWID
Oil Electricity	Electricity generation from oil	Terawatt hours	OWID
Fossil Fuel Electricity	Electricity generated from oil, gas and coal	Terawatt hours	OWID
Energy	Primary energy consumption	Kilowatt Hours	OWID
Temperature	Average mean surface-air temperature	Celsius	CCKP
Precipitation	Average precipitation	mm	CCKP

Table 2: Variable Summaries: Climate Damages Estimates Data

Figure 7, figure 8, and figure 9 show the distribution of each of the aforementioned variables, which are generally symmetric with slight skews. Notably, the temperature data exhibit a left skew, while the precipitation data display a heavy right skew.[5]

2.2   Natural Capital CES Estimation

In this subsection, we outline the methodologies employed to estimate the CES production functions and situate our findings within the broader literature. CES production functions have a prominent place in applied economics, as comprehensively reviewed by Lagomarsino (2020). Recent studies, including Papageorgiou et al. (2017), Jo (2022), and Jo and Miftakhova (2024), have explored the substitutability between clean and dirty energy inputs in production, building on the foundational work of Acemoglu et al. (2012), which examines the interplay between economic growth and pollution. Additionally, CES functions and their nested variants are integral to widely-used climate general equilibrium models such as DICE (e.g. Nordhaus (2008)) and Emissions Prediction and Policy Analysis Model (EPPA) (e.g. Jacoby, Reilly, McFarland, and Paltsev (2006)).

In this paper, we introduce a CES production function with a three-layer structure. The first layer assesses the substitution between produced, human and various natural capitals. The second layer decomposes energy production, represented by electricity generation, into contributions from fossil fuels and renewable energy sources. The third layer further disaggregates fossil energy-based electricity generation into output derived from coal, gas, and oil inputs.

The CES production function is highly non-linear, and its direct estimation necessitates either a linear

---

[5]The skewness is largely driven by the warm climates in East Asia and the Pacific, Latin America and the Caribbean in the case of temperature, and by the dry conditions in the Middle East and North Africa in the case of precipitation.

approximation or the use of non-linear estimation techniques. Kmenta (1967) introduced a linear approximation of the CES using a second-order Taylor series expansion around $\rho = 0$, which can be estimated using ordinary least squares (OLS). This method assumes an expansion around unitary elasticity of substitution, similar to a Cobb-Douglas production function. However, as Thursby and Lovell (1978) discuss, if ρ deviates significantly from 0, the approximation error can increase. Furthermore, Hoff (2004) highlights that Kmenta's results do not directly hold when there are more than two inputs, with the relevant parameter restrictions becoming increasingly complex as the number of inputs rises. On the other hand, non-linear methods have traditionally encountered convergence issues, and as noted by Henningsen and Henningsen (2012), they may yield economically meaningless parameter estimates. These issues typically arise when estimates fall outside the bounds prescribed by economic theory for each parameter.

An alternative approach to estimating CES production functions, although not applied in this paper, is the "indirect approach", which involves cost minimization (or profit maximization) and estimating the elasticity of substitution from the logarithm of the ratio of input prices. While the indirect approach is widely used,[6] it assumes exogenous prices, undistorted markets, and constant returns to scale—conditions that cannot be estimated within this framework. Given that price data for these natural capitals are unavailable and considering the significant issues raised by Feldstein (1967) and Papageorgiou et al. (2017) regarding these assumptions, we do not employ the indirect approach.

Instead, we implement both non-linear least squares (NLS) and the Kmenta approximation to balance the limitations of each method. We apply NLS to estimate all layers of the CES production function and, following Hoff (2004)'s recommendation, we use the Kmenta approximation, which relies on OLS, for the second and third layers, as both have only two inputs.[7] For NLS, we utilize two different methods. First, we implement Sequential Quadratic Programming (SQP) because it allows for constrained non-linear optimization, ensuring that the parameter values adhere to economic theory. This explicit introduction of constraints limits convergence issues, unlike the normalisation method used by Qian, Wu, and Fan (2018), which is less robust given our data. Second, we implement Adaptive Moment Estimation (Adam), a stochastic gradient descent method introduced by Kingma and Ba (2017) and is implemented using Tensorflow, a popular machine learning library.[8] Additionally, for the second and third layers, we introduce a third specification as a robustness check: we fix the returns to scale parameter, estimated using OLS, for the NLS estimation, as suggested by Corbo (1976) and Maddala and Kadane (1967), who demonstrate that the

---

[6]See Lagomarsino (2020) for a comprehensive list of literature employing the indirect approach and other methods.

[7]For the CES estimation, we aggregate Oil and Gas and treat them as a single factor.

[8]An introduction to Adam and our treatment of the method please refer to Appendix B

Kmenta approximation provides reliable estimates for the returns to scale parameter.

2.2.1   Results: First Layer

For the first layer, we estimate a CES production function using produced capital, human capital, and the following forms of natural capital: forest ecosystem services, cropland, minerals, and energy. We estimate the shares for these inputs by applying NLS to the equation below, where $Y_{i,t}^K$ is produced capital for country i at time t, $Y_{i,t}^{AL}$ is human capital (A is labor-augmenting technology), the natural capitals are denoted by $Y_{i,t}^k$. g_Y serves as a scaling parameter, θ are the share parameters, ρ_Y is the substitution parameter, and υ_Y is the return to scale parameter.

$$\ln(Y_{i,t}^T) = \ln(g_Y) - \left(\frac{\upsilon_Y}{\rho_Y}\right) \ln \left(\theta_{\mathrm{K}}(Y_{i,t}^K)^{-\rho_Y} + \theta_{AL}(Y_{i,t}^{AL})^{-\rho_Y} + \sum_k \theta_k (Y_{i,t}^k)^{-\rho_Y} \right) \tag{2}$$

Table 3 below shows that the results are similar across the two estimation methods and their specifications. Aligned with standard macroeconomic literature we observe, under all estimation specifications, that the share of human capital is the largest, followed by produced capital and natural capital related to energy. The elasticities of substitution presented below pertains to our global model and reflects a composite measure derived from varying elasticities across different countries. These estimates are novel as they introduce the elasticities of substitution between produced capital, human capital, and the various natural capitals, which has not been explored previously in the literature.

The estimated elasticity of substitution between these inputs, given by $\theta = \frac{1}{1+\rho_Y}$, ranges between 1.65 and 1.79. This range is lower than the 2 to 3 range found in studies by Papageorgiou et al. (2017) and Qian et al. (2018) for elasticities of substitution between energy and non-energy industries, which are the closest comparisons to our own results. This difference may be attributed to the functional form of the CES used. For instance, Papageorgiou et al. (2017) employs a production function that is a CES of different energies and a Cobb-Douglas function for capital, labor, and aggregate energy inputs. When we estimate a CES production function that integrates composite forms, akin to Papageorgiou et al. (2017) and Qian et al. (2018), by incorporating produced and human capital into a Cobb-Douglas production function $F(K, AL)$ - which then serves as an input into the CES - we find that the elasticity of substitution ranges between 2.54 and 2.57, as shown in table 13. This finding aligns more closely with the aforementioned studies. However, we argue that a CES specification with $F(K, AL)$ as one of its inputs imposes constraints on the substitutability between natural capitals and produced or human capital. Given that both produced and

human capital are essential in conjunction with various natural capitals to determine total production in an economy, estimates of the elasticity of substitution may be overstated.

Our estimates as well as the ones in literature suggest that one can substitute between produced capital, human capital and the different natural capitals. This may be the case since our estimates reflect a representative economy over the long run where the advent and proliferation of new adaptive technology can help promote substitutability between different inputs. In fact, when doing a expanding-window estimation, we find that the elasticity of substitution increases with time as can be seen in Figure 10, lending some empirical support to the fact that improvement in adaptive technology results in higher elasticity of substitution.

Moreover, given the CWON is a panel dataset, we divided the countries by income quartiles to estimate their respective elasticities of substitution as shown in table 30 to understand what drives the representative elasticity of substitution estimated below. These results show particularly high elasticity of substitution for countries in the second and fourth quartiles however, the data is not apt for a region or income-based heterogeneity analysis.

	Estimation Method			
	SQP Fixed υ	ADAM Fixed υ	SQP	ADAM
θ_{K}	0.2196	0.2278	0.2470	0.2437
	(0.0196)	(0.0195)	(0.0198)	(0.0022)
θ_{AL}	0.4091	0.4261	0.5168	0.5182
	(0.0308)	(0.0293)	(0.0372)	(0.0300)
θ_{FO}	0.0397	0.0366	0.0000	0.0002
	(0.0209)	(0.0204)	(0.0000)	(0.0000)
θ_{L}	0.1260	0.1178	0.0528	0.0399
	(0.0157)	(0.0135)	(0.0214)	(0.0142)
θ_{M}	0.0307	0.0155	0.0000	0.0105
	(0.0163)	(0.0072)	(0.0072)	(0.0031)
θ_{E}	0.1749	0.1764	0.1834	0.1874
	(0.0111)	(0.0101)	(0.0162)	(0.0132)
ρ_Y	-0.4407	–	-0.3929	–
	(0.0401)	–	(0.0415)	–
λ_Y	–	0.3536	–	0.3387
	–	(0.0219)	–	(0.0226)
g_Y	0.3850	0.3565	0.3440	0.3413
	(0.0178)	(0.0147)	(0.0124)	(0.0086)
υ_Y	1.0000	1.0000	0.9553	0.9555
	–	–	(0.0044)	(0.0037)
$\theta = \frac{1}{1+\rho_Y}$	1.7879	1.7368	1.6473	1.6753
Observations	2,184	2,184	2,184	2,184
MSE	0.1031	0.1028	0.0977	0.0981

Note: The values in the parentheses are the standard errors for relevant parameters calculated by bootstrapping.

Table 3: First Layer CES Estimates

We also estimate a CES production function with produced capital, human capital, and energy natural capital as its inputs to derive parameters for a reduced form DICE-style framework (we use in the quantitative modeling section), allowing us to compare our model's results (with all natural capital) and a framework with energy only. As shown in table 4, we find that the elasticity of substitution between these three inputs ranges from 1.63 to 1.73, consistent with previous estimates. Additionally, we observe that human capital retains the highest share, followed by produced capital. Of particular note is that both SQP and Adam, which are two different methods, yield the same results. The same results are obtained despite starting at different initial points indicating the ability of the methods to identify the optimal region and lending credibility to the results.

	Estimation Method			
	SQP Fixed υ	ADAM Fixed υ	SQP	ADAM
θ_{K}	0.2531	0.2531	0.2524	0.2524
	(0.0220)	(0.0215)	(0.0228)	(0.0233)
θ_{AL}	0.5426	0.5426	0.5576	0.5576
	(0.0267)	(0.0227)	(0.0279)	(0.0229)
θ_{E}	0.2043	0.2043	0.1900	0.1900
	(0.0179)	(0.0138)	(0.0169)	(0.0137)
ρ_Y	-0.4211	–	-0.3878	–
	(0.0454)	–	(0.0395)	–
λ_Y	–	0.3514	–	0.3277
	–	(0.0255)	–	(0.0235)
g_Y	0.2739	0.2739	0.3263	0.3263
	(0.0060)	(0.0049)	(0.0076)	(0.0068)
υ_Y	1.0000	1.0000	0.9468	0.9468
	–	–	(0.0023)	(0.0025)
$\theta = \frac{1}{1+\rho_Y}$	1.7274	1.7274	1.6335	1.6335
Observations	2,184	2,184	2,184	2,184
MSE	0.1114	0.1114	0.0983	0.0983

Note: The values in the parentheses are the standard errors for relevant parameters calculated by bootstrapping.

Table 4: First Layer CES Estimates (Energy Only Model)

2.2.2   Results: Second Layer

For the second layer, we decompose $Y_{i,t}^{\mathrm{Energy}}$ from the first layer into renewable and fossil fuel energy inputs. Here, we use electricity demand as a proxy for output and include fossil electricity generation and renewable electricity generation as inputs[9]. With two inputs for this layer, we employ both the NLS methods as well as the Kmenta-approximation methods for estimation. The NLS estimation is applied to the following equation:

$$\ln(Y_{i,t}^E) = \ln(g_E) - \left(\frac{\upsilon_E}{\rho_E}\right) \ln\left(\sigma_{FE}(Y_{i,t}^{FE})^{-\rho_E} + \sigma_{RE}(Y_{i,t}^{RE})^{-\rho_E}\right) \tag{3}$$

Whereas, we use OLS with country fixed effects denoted by μ_i and robust standard errors to estimate

---

[9]We do not use total electricity generation as our output because it is a simple linear sum of fossil electricity and renewable electricity generation, which would render CES estimation unfeasible.

the Kmenta-approximation, which follows this standard Taylor expanded expression:

$$\ln(Y_{i,t}^E) = \beta_0 + \beta_1 \ln(Y_{i,t}^{FE}) + \beta_2 \ln(Y_{i,t}^{RE}) + \beta_3 \left(\ln(Y_{i,t}^{FE}) - \ln(Y_{i,t}^{RE}) \right)^2 + \mu_i \tag{4}$$

Whereby

$$\beta_0 = \ln(g_E)$$

$$\beta_1 = \upsilon_E \sigma_{FE}$$

$$\beta_2 = \upsilon_E \sigma_{RE}$$

$$\beta_3 = \frac{-\upsilon_E \rho_E \sigma_{FE} \sigma_{RE}}{2}$$

The number of observations is lower with OLS due to missing values arising from taking logarithms of zero. Across all specifications detailed in table 5, we find that the share of fossil energy inputs in determining total energy output is consistently higher than that of renewable energy inputs, although these shares vary. These findings align with those reported by Papageorgiou et al. (2017), who observed that "clean" energy inputs account for approximately 45 percent of the total share, also with variations across specifications. Furthermore, the elasticities of substitution presented below for our specifications fall within the range estimated by Qian et al. (2018), who examined various nesting structures and found that 31 percent of their estimated elasticities of substitution between clean and dirty energy inputs fell within the range of 2 to 6. Notably, 35.9 percent of their estimates were between 0 and 1, while 22.7 percent were between 1 and 2, highlighting the robustness of our results. Papageorgiou et al. (2017) reported elasticities of substitution between clean and dirty energy ranging from 1.73 to 2.81, depending on the inputs used in their production function. Our estimates using the Kmenta-approximation and NLS with fixed returns to scale parameters are consistent with their findings[10]. Additionally, Jo (2022) found using the "indirect approach" that the elasticity of substitution between clean and dirty energy ranges from 1.9 to 3, while Jo and Miftakhova (2024) estimated it could be as high as 5, providing further support for our estimates.

---

[10]Results of the second layer OLS estimation are available in table 14

	Estimation Method				
	SQP	ADAM	Kmenta-OLS	SQP Fixed υ	ADAM Fixed υ
σ_{FE}	0.5542	0.5358	0.5076	0.5736	0.5226
	(0.0064)	(0.0639)	(0.0540)	(0.0061)	(0.0602)
σ_{RE}	0.4458	0.4642	0.4924	0.4264	0.4774
	(0.0064)	(0.0639)	(0.0540)	(0.0061)	(0.0602)
ρ_E	-0.8241	–	-0.4171	-0.5804	–
	(0.0280)	–	(0.0136)	(0.0259)	–
λ_Y	–	0.5907	–	–	0.5905
	–	(0.0047)	–	–	(0.0042)
g_E	2.6596	1.0322	4.0316	3.7000	1.0473
	(0.0452)	(0.0358)	(0.0575)	(0.0648)	(0.0332)
υ_E	0.9518	0.9445	0.8126	0.8126	0.8126
	(0.0048)	(0.0314)	(0.0117)	-	-
$\sigma = \frac{1}{1+\rho_E}$	5.6850	5.1329	1.7156	2.3832	5.1256
Observations	3,478	3,478	2,911	3,478	3,478
MSE	0.2025	0.0115	0.0186	0.3023	0.0153
Country Fixed Effects	No	No	136	No	No

Note: Carrying out further cleaning of the data such as removing countries with more than fifteen zero values for either input or output, the NLS estimated shares become more equitable, ρ_E = -0.7840 and MSE = 0.068. This demonstrates that the results are sensitive to the cleaning method applied. The values in the parentheses are the standard errors for relevant parameters calculated by bootstrapping.

Table 5: Second Layer CES Estimates

2.2.3 Results: Third Layer

For the third layer, we decompose fossil energy into three constituent components: oil, gas, and coal production. We use fossil electricity generation as our output variable, noting that it is a linear sum of coal, oil, and gas electricity generation and therefore these cannot be used as inputs. Recognizing that fossil electricity generation is primarily influenced by gas and coal inputs, we aggregate oil and gas production into a single input. All variables used in this analysis are measured in terawatt hours. By reducing the number of inputs from three to two, we apply both NLS and the Kmenta-approximation methods. The following expression is employed for the NLS estimation:

$$\ln(Y_{i,t}^{FE}) = \ln(g_F) - \left(\frac{\upsilon_F}{\rho_F}\right) \ln\left(\epsilon_G (Y_{i,t}^{G})^{-\rho_F} + \epsilon_C (Y_{i,t}^{C})^{-\rho_F}\right) \tag{5}$$

While we employ the following expression for the Kmenta-approximation, utilizing the same parameter interpretation as discussed for the second layer's estimates[11]:

$$\ln(Y_{i,t}^{FE}) = \beta_0 + \beta_1 \ln(Y_{i,t}^{G}) + \beta_2 \ln(Y_{i,t}^{C}) + \beta_3 (\ln(Y_{i,t}^{G}) - \ln(Y_{i,t}^{C}))^2 + \mu_i \tag{6}$$

Table 6 presents the varying shares of the oil-gas composite and coal production in determining fossil electricity generation across NLS and OLS methods, with both NLS methods assigning greater and equal weight to coal production and OLS assigning equal weights. However, data on electricity production by different fossil fuels[12] suggests that oil and gas collectively contribute between 30 percent to 40 percent to global fossil electricity generation, with the remainder being coal, aligning closely with the NLS results below. These findings are innovative and indicate moderate substitutability between different energy sources, reflecting constraints imposed by existing infrastructure capabilities. It is important to highlight that the scaling parameter g_F is notably large due to some countries being net importers of fossil fuel-generated electricity, enabling better alignment with observed data.

Furthermore, as with the first layer, the OWID Energy dataset is disaggregated by countries and as such, we estimated the elasticities of substitution for the second and third layer using both NLS and OLS as seen in table 30 and table 31 to try decompose the representative elasticities of substitutions estimated for the two layers. However, the data is not suitable for analyzing income-level heterogeneity in this context.

---

[11]Third layer OLS results are available in table 15.

[12]See Our World in Data: Energy Mix

	Estimation Method				
	SQP	ADAM	Kmenta-OLS	SQP Fixed v	ADAM Fixed v
ϵ_G	0.3721	0.3216	0.5013	0.3490	0.3990
	(0.0235)	(0.0770)	(0.0512)	(0.0411)	(0.)
ϵ_C	0.6279	0.6042	0.4924	0.6510	0.6010
	(0.0235)	(0.0770)	(0.0512)	(0.0411)	(0.0127)
ρ_F	-0.2132		-0.2162	-0.1154	–
	(0.0421)	–	(0.1014)	(0.0645)	–
λ_Y	–	0.1898	–	–	0.3365
	–	(0.0760)	–	–	(0.0187)
g_F	63.1597	1.0881	52.1997	61.2087	1.2630
	(3.0919)	(0.0673)	(0.2446)	(3.2124)	(0.0399)
v_F	0.6167	0.8021	0.4149	0.4149	0.4149
	(0.0207)	(0.1713)	(0.0425)	–	–
$\epsilon = \frac{1}{1+\rho_F}$	1.2710	1.4250	1.2643	1.1305	1.6670
Observations	1,152	1,152	1,152	1,152	1,152
MSE	1.9954	0.0150	0.1326	2.2420	0.0075
Country Fixed Effects	No	No	48	No	No

Note: The values in the parentheses are the standard errors for relevant parameters calculated by bootstrapping.

Table 6: Third Layer CES Estimates

2.3   Natural Capital Climate Damages Estimation

In this section, we present novel estimates of the impact of temperature on the considered natural capitals.

2.3.1   Identification Strategy

The estimation of climate damages in this study aligns with the latest advancements in climate econometrics literature, which have notably progressed over the past two decades[13]. The current methodological frontier includes panel data analysis, leveraging plausibly random variations in weather with spatial and time fixed effects (Hsiang, 2016). In this context, two primary approaches have emerged to ascertain the causal impact of temperature on socioeconomic factors: yearly average temperature and temperature bins[14]. In this study, we adopt the former approach as it aligns more coherently with the climate damages incorporated

---

[13]The literature has evolved from cross-country studies (Nordhaus, 2006) to panel data approaches (Dell et al., 2012; Burke et al., 2015; Kotz et al., 2024), enabling more precise estimates through the identification of effects from idiosyncratic weather shocks (Hsiang, 2016).

[14]The former method estimates the impact of changes in yearly average temperature (Dell et al., 2012; Burke et al., 2015), whereas the latter evaluates the impact of an additional day with average temperature within a specific range (Deschênes, Greenstone, and Guryan, 2009; Carleton et al., 2022).

into our macroeconomic model presented in the next section.[15]

Our empirical strategy adopts an agnostic approach towards model selection, aiming to identify the most appropriate model guided by empirical evidence aligned with the objectives of this paper. Hence, we define each variable of interest as a flexible function of temperature and precipitation:

$$y_{i,t} = g(T_{i,t}) + f(P_{i,t}) + \sum_{\ell \geq 1} h(T_{i,t-\ell}) + \delta_i + \lambda_t + \varepsilon_{i,t} \tag{7}$$

where $y_{i,t}$ represents the natural logarithm of country i's variable of interest in year t, $g(T_{i,t})$ denotes a flexible function capturing the impact of yearly average temperature on $y_{i,t}$ for country i in year t, $f(P_{i,t})$ represents a flexible function capturing the impact of yearly total precipitation on $y_{i,t}$, $\sum_{\ell \geq 1} h(T_{i,t-\ell})$ is defined as the sum over ℓ lags of a flexible function of yearly average temperature, δ_i stands for a country fixed effect that accounts for country-specific unobserved constant components, λ_t denotes a year fixed effect that accounts for time-specific unobserved constant components such as economic and climate trends or shocks, and $\varepsilon_{i,t}$ represents the autocorrelated and spatially correlated error component.

The relevant literature has not yet reached a consensus on which specification better identifies the general model defined in equation (7). Specifically, there is disagreement on how the dependent and independent variables should enter the model (i.e., in levels or first differences), and on the functional form of $f(\cdot)$ and $g(\cdot)$ (i.e., linearly or as higher-order polynomials). Regarding the first point, Burke et al. (2015) argue in their seminal paper that the GDP series is nonstationary, hence it should enter the estimation in first differences. Newell, Prest, and Sexton (2021) argue that the temperature series is also nonstationary, hence it should enter the model in first differences as well. Given the several variables in our model, we cannot assert a priori whether they are stationary or not. Therefore, we empirically test this argument using data.

Appendix B.0.1 reports the results of the Augmented Dickey-Fuller unit-root test[16] for all variables used in the empirical analysis. Initially, we test the variables of interest and subsequently apply the tests on the remaining detrended variables for which we did not reject the null hypothesis of nonstationarity in the first stage. We reject the null hypothesis in the test without trends for temperature, precipitation, minerals, and cropland, as well as in the test accounting for trends for forest ecosystems, gas, oil, fossil fuels, and renewable energy, indicating that these variables are either stationary or trend stationary. Conversely, we fail to reject the null hypothesis for coal and aggregate energy, which are found to be nonstationary. Therefore, we

---

[15]For a discussion on these methodologies in the context of economic damages, refer to Tarsia (2023).

[16]We use the Inverse chi-squared and Modified inverse chi-squared statistics, which are more suitable for large panels (Choi, 2001).

estimate the model from equation (7) in levels for the stationary variables and in first differences for the nonstationary variables[17].

Regarding the specification of the damage functions $f(\cdot)$ and $g(\cdot)$, we depart from the quadratic model from Burke et al. (2015) and opt for a linear model as in Dell et al. (2012). Linear in this context refers to the order of the temperature term polynomial included in the reduced form estimation. The damage function included in the model remains non-linear as all the dependent variables are taken in logs. We do this for two reasons. First, the aim of this section is to estimate climate damages which can be used in our macroeconomic model simulation. Since the model requires global-level estimates, we consider the linear model to be better suited, as we are interested in the global average marginal effect rather than how different countries are impacted by higher temperatures. Second, the results from the models including the quadratic terms reported in section D show that the quadratic term in the second order polynomial function is often not statistically significant.

An additional aspect often discussed in the literature concerns the persistence of temperature shocks identified through lagged effects (i.e., levels versus growth effects). Kotz et al. (2024) elaborate on disentangling these effects to identify the persistence of climate impacts on economic growth using multiple lags of temperature. Given the scope of this paper and the limited time dimension of our data, we include two lags of temperature in our model.

Therefore, we estimate the marginal effect of an additional $1°C$ in yearly average temperature on our variables of interest using the following model:

$$y_{i,t} = \alpha + \beta_0 T_{i,t} + \sum_{\ell=1}^{2} \beta_\ell T_{i,t-\ell} + \psi_0 P_{i,t} + \delta_i + \lambda_t + \varepsilon_{i,t} \tag{8}$$

where the variables are defined as in equation (7). In this framework $y_{i,t}$ is the log of the various natural capital variables of interest, defined in levels if stationary or in first difference otherwise, according to the results of appendix B.0.1. The marginal effects identified by the estimates β_ℓ are the average percentage change in $y_{i,t-\ell}$ due to an additional $1°C$ in yearly average temperature $T_{i,t-\ell}$ for $\ell = \{0, 1, 2\}$.

2.3.2 Results

This section reports the empirical estimates arising from the analysis based on equation (8) for each of the variables of interest. For presentation reasons, we divide the variables between table 7 for the variables

---

[17]The marginal effect of an additional $1°C$ in year t that we identify, $\frac{\partial Y_{i,t}}{\partial T_{i,t}}$, is consistent between the two estimation methods.

belonging to the first layer (i.e. produced capital, cropland, forest ecosystem, minerals, aggregate energy) and table 8 for the variables belonging to the second and third layers (coal, gas, oil, fossil fuel, and renewable energy). As is evident, all variables apart from oil (column 6) are negatively impacted by higher temperature, although with different timing. At this stage, it is important to clarify that the estimates in this paper reflect the impact of a $1°C$ increase, whereas yearly average temperatures typically fluctuate by only a fraction of a degree.

The estimates are negative and statistically significant in all lags $\ell = \{0, 1, 2\}$ for produced capital (column 1), gas (column 7) and fossil fuel (column 9), in lags $\ell = \{0, 1\}$ for forest ecosystem (column 3), in lags $\ell = \{1, 2\}$ for cropland (column 2) and minerals (column 4), and only in lag $\ell = 0$ for aggregate energy (column 5) and renewable energy (Column 10). The estimates for coal (column 6) are statistically significant only in period $t - 2$, and surprisingly positive. However, since the contemporaneous (period t) estimate is negative, the positive estimate indicates the presence of the so-called sign reversal, suggesting the absence of persistent growth effects for this variable. Since the estimates for coal are inconsistent with those for the other variables and are not statistically significant, we decide to rely on the estimates for fossil fuel in the coal-specific damage function of our model.

	(1)	(2)	(3)	(4)	(5)
	Produced Capital	Cropland	Forest Ecosystem	Minerals	ΔAgg. Energy
T	-0.0297**	-0.015	-0.011**	-0.027	
	(0.0084)	(0.012)	(0.0036)	(0.017)	
$(\ell 1)T$	-0.0396***	-0.051***	-0.011**	-0.082**	
	(0.0088)	(0.0081)	(0.0038)	(0.026)	
$(\ell 2)T$	-0.0357***	-0.047***	-0.0078	-0.16***	
	(0.0086)	(0.010)	(0.0070)	(0.027)	
ΔT					-0.016***
					(0.0035)
$(\ell 1)\Delta T$					-0.0056
					(0.0034)
$(\ell 2)\Delta T$					-0.0013
					(0.0024)
P	0.00001	0.0001	-0.00001	0.0001	
	(0.00002)	(0.00006)	(0.00002)	(0.0001)	
ΔP					0.00001
					(0.00001)
Country FE	Yes	Yes	Yes	Yes	Yes
Year FE	Yes	Yes	Yes	Yes	Yes
R^2	1.00	1.00	1.00	0.93	0.26
N	1584	1584	1562	1254	1512

Standard errors in parentheses

* $p < 0.10$, ** $p < 0.05$, *** $p < 0.01$

Table 7: Point estimates and standard errors from the regressions of weather variables on the natural capital variables belonging to the first layer. Results from the linear model of temperature with all variables expressed in differences, country and year FE, and standard errors clustered at the regional level as identified by the World Bank.

The estimates are generally coherent across variables, showing that different sources of natural capital are consistently negatively affected by increasing temperatures. Nevertheless, the magnitude of climate damages varies across variables. Among the variables belonging to the first layer reported in table 7 the marginal effect of an additional $1°C$ in yearly average temperature ranges between approximately -1% for forest ecosystem and aggregate energy to approximately -8% for minerals (in year $t-1$), whereas the marginal effect is approximately -3% across all years for produced capital and approximately -5% for cropland (in years $t-1$ and $t-2$). The estimates for the variables belonging to layers two and three are characterised on average by higher magnitude. The marginal effects range from between -4% and -6% for fossil fuel, and between -8% and -10% for gas, whereas the effect is approximately -6% for renewable energy (in year t).

	(6) ΔCoal	(7) Gas	(8) Oil	(9) Fossil Fuel	(10) Renewable Energy
T		-0.084**	-0.041	-0.063**	-0.062**
		(0.029)	(0.048)	(0.020)	(0.020)
$(\ell 1)T$		-0.088***	-0.011	-0.057**	-0.029
		(0.023)	(0.051)	(0.019)	(0.018)
$(\ell 2)T$		-0.098***	0.031	-0.039**	-0.045
		(0.017)	(0.032)	(0.015)	(0.024)
ΔT	-0.0037				
	(0.020)				
$(\ell 1)\Delta T$	0.021				
	(0.018)				
$(\ell 2)\Delta T$	0.014**				
	(0.0041)				
P		-0.0003**	-0.0004*	-0.0001	0.0002**
		(0.0001)	(0.0002)	(0.0001)	(0.0001)
ΔP	-0.00011**				
	(0.00004)				
Country FE	Yes	Yes	Yes	Yes	Yes
Year FE	Yes	Yes	Yes	Yes	Yes
R^2	0.14	0.92	0.89	0.97	0.96
N	1067	1452	1423	1504	1483

Standard errors in parentheses

* $p < 0.10$, ** $p < 0.05$, *** $p < 0.01$

Table 8: Point estimates and standard errors from the regressions of weather variables on our the natural capital variables belonging to the second and third layers. Results from the linear model of temperature with all variables expressed in differences, country and year FE, and standard errors clustered at the regional level as identified by the World Bank.

Furthermore, these effects are generally non-transitory and persist over time, as shown by the negative and statistically significant estimates for lagged temperature. Since, apart from coal, the estimates for the other variables are negative or not statistically significant, the cumulative effect of temperature is negative, highlighting the presence of persistent growth effects. This implies that the average negative shocks on natural capital induced by higher temperature are not recovered, but instead affect countries' ability to grow. This result is not surprising given the variables we are analysing. Unlike GDP analysed in previous work, natural capital is not as dynamic and regenerates at slow rates. Therefore, any negative shock is unlikely to be recovered in the medium term by definition.

Rising temperatures adversely affect natural capital through several key mechanisms. For cropland, which encompasses total arable land, increased temperatures can lead to soil degradation, reduced water

availability, and higher evaporation rates. As soil degradation and desertification spread, some regions will become unsuitable for cultivation, leading to a reduction in the total area of arable land. These changes diminish the land's capacity to support agricultural activities, ultimately impacting food production and economic stability in agrarian regions. Moreover climate change is projected to alter land conditions with feedbacks on regional climate to the extent that changes in land conditions impacts warming and affects the intensity, frequency and duration of extreme events, further exacerbating land-related climate damages (IPCC, 2019).

Forest ecosystems, vital for carbon sequestration and biodiversity, are particularly vulnerable to temperature increases (Graham, Turner, and Dale, 1990). Elevated temperatures intensify evapotranspiration and moisture stress, weakening trees and making forests more susceptible to fires, pests, and diseases (Seidl, Thom, Kautz, Martin-Benito, Peltoniemi, Vacchiano, Wild, Ascoli, Petr, Honkaniemi, et al., 2017). The resulting decline in forest cover compromises ecosystem services and exacerbates the impacts of climate change.

Mineral resources availability is also negatively impacted by rising temperatures. Higher temperatures can increase cooling costs in mining operations, reduce the efficiency of power plants, and disrupt energy transmission infrastructure. The physical processes involved in extracting and processing minerals become less efficient under extreme heat, leading to higher operational costs and reduced output. Despite its significance, this issue has not been fully addressed in the existing literature.

The study further highlights the vulnerabilities of fossil fuels—coal, gas, and oil. Higher temperatures can decrease the efficiency of fossil fuel extraction and processing, while increasing the risk of disruptions due to extreme weather events. This not only raises the costs associated with fossil fuel production but also impacts the stability of energy supplies. Moreover, changing climate and weather conditions can also influence the supply of renewable energy, specifically for the hydro and wind power generation. For a review of the various dynamics climate change can affect energy supply see Schaeffer, Szklo, de Lucena, Borba, Nogueira, Fleming, Troccoli, Harrison, and Boulahya (2012). Furthermore, climate change-induced higher temperatures can influence the demand for energy consumption, particularly in the short term. Warmer years result in increased energy consumption due to greater cooling requirements during warm months, while simultaneously reducing energy demand for heating in colder months. The net effect of these opposing forces depends on the intra-annual distribution of daily temperatures and the degree of seasonal variability.

The economic implications of these climatic impacts are extensive. Reduced agricultural capacity affects food security and increases volatility in food prices, with cascading effects on economies dependent on

agriculture. The decline in forest health and cover affects industries reliant on forest products and services, from timber to tourism. Increased operational costs in mining and energy sectors lead to higher prices for these essential resources, impacting a wide range of industrial activities and economic outputs.

3   The Model

In this section, we assess the impact of integrating natural capital into a standard macroeconomic framework with climate dynamics. The world economy is modeled as being managed by a social planner who internalizes the climate externality and accounts for all available natural capital resources. The planner efficiently allocates the economy's resources with the objective of maximizing the total welfare of the representative consumer.

The modeled world economy operates in discrete time with yearly time steps and over an infinite horizon. It features an infinitely lived representative household and a production sector that combines output from several capital types, each subject to climate damages. Final output is generated using a mix of capital, labor, and natural capital inputs, including energy, minerals, land, and forest ecosystem. Energy production can utilize either fossil fuels (oil, coal, and gas) or renewable resources.

In this framework, aggregate output is represented by a nested CES function, integrating produced capital and human capital (i.e., labor augmenting technology), and natural capital. Fossil fuel production introduces an environmental externality through CO_2 emissions, while renewable energy sources are emission-neutral (i.e., they do not emit CO_2). Emissions from fossil fuel production cause climate-related damages that affect all production components. A graphical representation of the modeling framework is displayed in figure 1.

We begin by outlining the climate dynamics, followed by the aggregate output production problem. We then address the household's optimization problem and conclude with the social planner's problem and present the SCC in our economy.

3.1   Climate Dynamics

Building on the foundations of standard integrated assessment models (IAMs) such as those proposed by Nordhaus (1991) and Nordhaus and Yang (1996), we integrate climate dynamics into our natural capital macroeconomic framework. We model the processes governing the atmospheric concentration of carbon dioxide and global temperature as follows. The global temperature T_t is assumed to be linearly proportional to the stock of CO_2 emissions, representing the cumulative emissions over time, as established by Matthews,

Gillett, Stott, and Zickfeld (2009):

$$T_{t+1} = \epsilon_t^T \phi_1(\phi_2 X_t - T_t) + T_t, \tag{9}$$

with ϕ_1 and ϕ_2 the climate transient parameters calibrated to both match temperature at the start of the simulation (i.e. 2018), and the temperature dynamics with respect to cumulative emissions and the initial.

Following Matthews et al. (2009), cumulative CO_2 emissions, denoted as X_t, reads as:

$$X_{t+1} = X_t + E_t, \tag{10}$$

ϵ_t^T is a temperature shock, which captures exogenous variations in temperature and is assumed to follow an AR(1) process $(log(\epsilon_t^T) = \rho_T log(\epsilon_{t-1}^T) + \eta_t^T)$ where ρ_T is the persistence of the shock and $\eta_t^T \sim N(0, \sigma^{T^2})$. X_{t+1} is the concentration of gases in the atmosphere, $E_t \geq 0$ anthropogenic emissions of CO_2 stemming from fossil fuel production Y_t^{FE} where:

$$E_t = \phi_E Y_t^{FE}. \tag{11}$$

where ϕ_E is the emission intensity to fossil energy output.

In the spirit of Nordhaus (1991), temperature damages production. However the novelty in our work, is that: i) temperature damages are specific to each input in our production function and ii) feature temperature lags. The damage function reads as:

$$d_h(\cdot) = \sum_m \beta_m^h T_{t-m}. \tag{12}$$

where β_m^h are the estimated betas for each natural capital. m represents temperature lags, while h represents all natural capital impacted by climate raising temperatures, namely: oil, gas, coal, renewable energy, minerals, cropland, forest ecosystem, as well as the capital/labour inputs.

3.2 Natural Capital and Production

The World Bank's Changing Wealth of Nations dataset classifies natural capital into nine categories: energy, minerals, land, forest ecosystem, timber provision, mangroves, fisheries, and protected areas. We focus on energy, minerals, land, and forest ecosystem, as well as the decomposition of energy resources.

We expand the traditional Cobb-Douglas production function with capital K_t and labor L_t to include the following natural capitals: energy Y_t^E, minerals Y_t^M, land Y_t^L, forest ecosystem services Y_t^{FO}, fossil energy

Y_t^{FE}, renewable energy Y_t^{RE}, oil Y_t^O, gas Y_t^G, and coal Y_t^G. The following subsections detail the nested CES structure of our model and the laws of motion for the various stocks in our economy.

3.2.1 First Layer CES: Final Output

Final output Y_t^T is a CES function of the following aggregates: (i) produced capital Y_t^K, (ii) energy Y_t^E, (iii) minerals Y_t^M, (iv) land Y_t^L, (v) forest ecosystem services Y_t^{FO}, and (vi) human capital (labour augmenting technology) Y_t^{AL}:

$$Y_t^T = \epsilon_t^A g_Y \left(\sum_k \theta_k \left(Y_t^k \right)^{\frac{\theta-1}{\theta}} \right)^{\frac{\theta}{1-\theta}}, \tag{13}$$

where $k \in \left\{ Y_t^{\text{K}}, Y_t^E, Y_t^M, Y_t^L, Y_t^{\text{FO}}, Y_t^{\text{AL}} \right\}$. θ_k represents the weight of each input (with $\sum_k \theta_k = 1$), while θ is the elasticity of substitution and g_Y a weight to final output. ϵ_t^A is a TFP shock and is assumed to follow an AR(1) process $(log(\epsilon_t^A) = \rho_A log(\epsilon_{t-1}^A) + \eta_t^A)$ where ρ_A is the persistence of the shock and $\eta_t^A \sim N(0, \sigma^{A^2})$.

Human capital production function reads as:

$$Y_t^{\text{AL}} = e^{d_{\text{AL}}(\cdot)} A_t L_t, \tag{14}$$

where A_t is labor augmenting productivity and L_t labour input, which is subject to an exogenous growth trend $\Gamma_t = \gamma^\Gamma \Gamma_{t-1}$.[18]

Natural capital production for minerals and land usage is assumed to rely on an exhaustible finite stock S_t^j of each natural capital, respectively (in the spirit of Van der Ploeg and Rezai (2021)). The possibility of discoveries (minerals) or transformations (land) is captured by D_t^j. Similarly, forest ecosystem services production relies on an exhaustible finite stock S, where D captures both investment and natural regeneration. Accumulation of non depreciated produced capital is possible via capital investments as it is standard in macroeconomic frameworks. This flexible specification allows us to represent the laws of motion for both renewable and non-renewable natural capital in the same form:

$$S_{t+1}^j = S_t^j - F(Y_t^j) + \epsilon_t^{D_i} \alpha_j D_t^j, \tag{15}$$

with: where $j \in \left\{ Y_t^K, Y_t^{FO}, Y_t^L, Y_t^M \right\}$ and $F(Y_t^j) = \delta_j S_t^j$ and α_j the share of discovery that is subject to an

---

[18]In the appendix we present both the balanced growth path equilibrium and the non-detrended economy equilibrium.

AR(1) shock $\epsilon_t^{D_i}$ [19]. Natural capital Y_t^j production is assumed to use the stock S_t^j and subject to non-linear climate damages $d_j(\cdot)$:

$$Y_t^j = e^{d_j(\cdot)} S_t^j. \tag{16}$$

3.2.2 Second Layer CES: Energy

Energy is a CES function of fossil energy and renewable energy:

$$Y_t^E = g_E \left(\sigma_{FE} \left(Y_t^{FE} \right)^{\frac{\sigma-1}{\sigma}} + \sigma_{RE} \left(Y_t^{RE} \right)^{\frac{\sigma-1}{\sigma}} \right)^{\frac{\sigma}{1-\sigma}}, \tag{17}$$

with Y_t^{FE} and Y_t^{RE} the production of fossil and renewable energy, respectively. σ_{FE} and σ_{RE} represents the weight of each input (with $\sigma_{FE} + \sigma_{RE} = 1$), while σ is the elasticity of substitution and g_E a weight to aggregate energy output.

As with the other types of natural capital, renewable energy production relies on a finite stock S_t^{RE}. This stock can be increased through investment D_t^{RE} and part of it is used in the production process:

$$S_{t+1}^{RE} = S_t^{RE} - F(Y_t^{RE}) + \epsilon_t^{D_{RE}} \alpha_{RE} D_t^{RE}, \tag{18}$$

with α_{RE} the share of renewable investment, $\epsilon_t^{D_{RE}}$ and AR(1) investment shock, and $F(Y_t^{RE}) = \delta_{RE} S_t^{RE}$. Renewable energy production Y_t^{RE} is again assumed to use the stock S_t^{RE} and is subject to idiosyncratic climate damages d_{RE}:

$$Y_t^{RE} = e^{d_{RE}(\cdot)} S_t^{RE}. \tag{19}$$

3.2.3 Third Layer CES: Fossil Energy

Fossil energy is, in turn, a CES function of oil, gas, and coal:

$$Y_t^{\text{FE}} = g_F \left(\sum_i \epsilon_i \left(Y_t^i \right)^{\frac{\epsilon-1}{\epsilon}} \right)^{\frac{\epsilon}{1-\epsilon}}, \tag{20}$$

where $i \in \left\{ Y_t^O, Y_t^G, Y_t^C \right\}$. ϵ_{FE} and ϵ_i represents the weight of each input (with $\epsilon_O + \epsilon_G + \epsilon_C = 1$), while ϵ is the elasticity of substitution between oil, gas, and coal, and g_F a weight to aggregate fossil energy output.

[19]The AR(1) shock to discovery reads as: $log(\epsilon_t^{D_j}) = \rho_D log(\epsilon_{t-1}^{D_j}) + \eta_t^{D_i}$, with $\eta_t^{D_i} \sim \mathcal{N}(0, \sigma_{D_j}^2)$

Similar to the previous natural capitals, oil, gas, and coal each have a finite stock S_t^i, but discoveries D_t^i can be made over time, allowing these natural capital stocks to increase overtime:

$$S_{t+1}^i = S_t^i - F(Y_t^i) + \epsilon_t^{D_i} \alpha_i D_t^i, \tag{21}$$

with $\epsilon_t^{D_i} \alpha_i$ the stochastic share of discovery as for the first layer, and $F(Y_t^i) = \delta_i S_t^i$ and natural capital Y_t^j production is assumed to use total stock S_t^i and subject to the same type of climate damages discussed above:

$$Y_t^i = e^{d_i(\cdot)} S_t^i. \tag{22}$$

3.3 Households

The representative household problem is approached using a CRRA utility function with habits formation:

$$\text{Welfare}_t = E_0 \sum_{t=0}^{\infty} \beta^t \left\{ \frac{(C_t - \gamma_H H_t)^{1-\sigma^H}}{1 - \sigma^H} \right\}, \tag{23}$$

where β represents household time preference and σ^H is the risk aversion parameter. We introduce γ_H a zero steady state value of the utility function under the non-detrended version of the model.[20]

The household derive utility from consumption expenditures C_t subject to habit formation H_t and inelastic labor hours $\frac{L_t}{\Gamma_t} = \bar{L}$.

$$H_{t+1} = mH_t + (1 - m)C_t. \tag{24}$$

where m is the level of habits formation. As argued in Benmir, Jaccard, and Vermandel (2020), to maximize the model's ability to generate realistic asset pricing and macroeconomic implications, we introduce internal habit formation. Furthermore, habits lead to higher volatility in carbon pricing compared to standard CRRA utility or recursive preferences. This higher volatility over the business cycle have important implication with respect to policy design and optimal carbon over the business cycle.

---

[20]We set γ_H close to 1.

3.4 The Aggregate Resource Constraint

We close the model with the aggregate resource constraint of the economy, which reads as follows:

$$Y_t^T = C_t + \sum_h D_t^h. \tag{25}$$

3.5 The Social Cost of Carbon Under The Presence of Natural Capital

We now characterize the first-best allocation, considering the optimal plan a benevolent social planner would choose to maximize welfare.[21]

Definition 1 *The optimal policy problem for the social planner is to maximize total welfare in equation* (23) *by choosing a sequence of allocations for the quantities* $\{H_{t+1}, X_{t+1}, T_{t+1}, C_t, E_t, Y_t^{AL}, Y_t^{FE}, Y_t^E, Y_t^T, Y_t^h, D_t^h, S_{t+1}^h\}$, *for given initial conditions for the eleven endogenous state variables* H_0, S_0^h[22], T_0 *and* X_0 *as well as all the stochastic shocks that satisfy equations* (9), (10), (11), (13), (14), (15), (16), (17), (18), (19), (20), (21), (22), (24).

Proposition 1 *In a centralized equilibrium, the planner fully internalizes the SCC (i.e. the shadow price of* CO_2 *emission* V_t^E, *ensuring that the marginal cost of emissions matches the shadow price of* CO_2 *emissions.*

Solving the optimal policy problem, the SCC under the presence of natural capital reads as:

$$V_t^E = \beta E_t \left\{ \frac{\lambda_{t+1}^C}{\lambda_t^C} \left[V_{t+1}^E + \epsilon_{t+1}^T \phi_1 \phi_2 V_{t+1}^T \right] \right\}, \tag{26}$$

where V_t^T represents the discounted sum of future temperature climate damages:

$$V_t^T = E_t \left\{ \beta \frac{\lambda_{t+1}^C}{\lambda_t^C} \left[(1 - \epsilon_{t+1}^T \phi_1) \right] V_{t+1}^T \right\}$$
$$- \sum_h \sum_m E_{t+m} \left\{ \left[\left(\prod_{o=0}^{m-1} \beta \frac{\lambda_{t+1+o}^C}{\lambda_{t+o}^C} \right) \Psi_{t+m}^h \beta_m^h Y_{t+m}^h \right] \right\}. \tag{27}$$

---

[21]Refer to the appendix for the full derivations.
[22]Where $h \in \{i\} \cup \{j\} \cup \{RE\}$

4 Quantitative Analysis

In what follows, we leverage the parameter estimates presented in section 2 to perform simulations using the model detailed in section 3. Throughout this section, we will compare the results of our model simulations with those of a simpler model that includes only produced capital, human capital, and energy as inputs to production. This simpler model is more common in the literature and serves as a benchmark for comparison, allowing us to highlight the various results we will be discussing.

4.1 Calibration

We start by explaining how we calibrate our model to represent the world using both our CES and climate damage estimates, as well as 2018 natural capital and GDP data from the World Bank and other data sources.

First, all climate damages,[23] CES elasticities of substitution for each of our different production function nests, CES shares, and CES weights are derived from our empirical estimates. Additionally, we perform a sensitivity analysis to demonstrate the impact these factors have on the various shadow prices.

Calibration of parameters with time intervals is conducted annually. Following conventional practice, we have customized the calibration process to match key observed aggregates, such as temperature, global CO_2 emissions, and the value of each natural capital stock, all within the world context. This meticulous calibration ensures that our model accurately captures the real-world dynamics and trends of these critical environmental and economic indicators. Table 27 summarizes the moments we match, while table 26 lists the values of all parameter calibrations.

The parameters pertaining to the business cycle structure of our model are conventional. For the standard parameters in these models, such as the discount factor β and the risk aversion σ^H, we align with typical values used in macroeconomic modeling. Specifically, the discount factor β is set at 0.968 to match a 3.3 percent world GDP-weighted interest rate, while the risk aversion σ^H is set at 2, following Stern (2008). Labour $\bar{L}$ hours worked are set at $1/3$ (which corresponds to daily mean of 8h). The productivity of labor A is calibrated to match the level of human capital in 2018 as reported in the matching moments table (see table 27). The habits level parameter m is set at 0.9, following Benmir et al. (2020). The parameter γ_H takes two values: i) $\gamma_H = 1$ in the case of stationary equilibrium (i.e., the discovery/investment exercise),

---

[23]The only exception being damages to human capital, which are calibrated following the standard DICE calibration of damages to output.

and ii) $\gamma_H = 0.975$ in the case of the non-detrended economy, to avoid utility going to zero with consumption equal to habits at the steady state. Finally, the AR(1) shock process persistence parameter is set at 0.9, as is standard in the literature, and the growth rate of the world economy γ^Γ is set at 3 percent, corresponding to the average world growth rate over the past 10 years.

All specific capital production values are set according to data taken from the World Bank database. In particular, parameters such as the weights for aggregating fossil energy, aggregate energy, and final outputs—denoted as g_F, g_E, and g_Y, respectively—are calibrated to match the values of Y^{FE}, Y^E, and Y^T presented in table 27.

We set the output of renewable energy to \$542.7 billion, based on the global average cost of electricity from renewable sources (\$81 per megawatt-hour, MWh) in 2018, relative to total production of 6,700,000,000 MWh.[24]

For the remaining specific outputs, which are set according to the World Bank, we use the production share of capital stocks, δ_s, to match the values in the corresponding data in table 27. Regarding discovery and investment, we use the discovery/investment share, α_s, to precisely match the level of discovery/investment relative to specific capital production in table 27.footnoteWe also consider cases where these intensity shares change unexpectedly in the context of our stochastic shock analysis. The ratio of discovery/investment to each specific capital production is calibrated using estimates from the International Energy Agency (IEA). In particular, the investment/discovery-to-output ratios for renewable energy, oil, gas, and coal are set to 156%, 0.46%, 0.14%, and 1%, respectively. For mining, land, and forest ecosystem services, the investment/discovery-to-output ratios are set to 3%.

In calibrating the climate block of the model, we follow Dietz and Venmans (2019) and set the parameters for the global temperature function as $\zeta_1^o = 0.50$ and ζ_2^o to retrieve the initial temperature level of 1^oC at the start of the transition. Finally, the emission intensity parameter ϕ_E is set to 0.0014 to match the initial state of emissions with respect to fossil fuel production.

4.2 Model Solution

To solve for the long-run pathway scenario, we use a perfect foresight algorithm, which allows us to integrate deterministic trends. This approach maintains the ability of deterministic methods to provide accurate

---

[24]The global total production of renewable energy in 2018 was between 6.7 and 7.4 petawatt-hours (PWh). The average price is based on the International Renewable Energy Agency (IRENA): i) onshore (\$50 to \$70 per MWh) and offshore (\$120 to \$150 per MWh) wind, ii) solar photovoltaic (\$85 per megawatt-hour), iii) hydropower (\$40 to \$80 per MWh), and iv) Bioenergy and Geothermal (\$70 to \$150 per MWh). See https://www.irena.org/-/media/Files/IRENA/Agency/Publication/2018/Apr/IRENA_Report_GET_2018.pdf?utm_source=chatgpt.com.

accounts of non-linearities, whereas usual local approximation techniques do not perform as well in the presence of such non-linearities. To address the short-term business cycle implications of discovery/investment volatility, we rely on second-order perturbation methods around the initial steady state to retrieve impulse response functions.

4.3 Shadow Prices Estimates

In this section, we present our estimates of the SCC as well as natural capitals shadow prices, contrasting the results from our natural capital macro framework with those from a standard DICE-style framework. In the latter, the final output Y_t^T is modeled as a simple CES function of produced capital, human capital, and energy.[25]

$$Y_t^T = \left(\gamma_K (Y_t^K)^{\frac{\theta-1}{\theta}} + \gamma_{FE}(Y_t^{FE})^{\frac{\theta-1}{\theta}} + \gamma_{AL}(Y_t^{AL})^{\frac{\theta-1}{\theta}} \right)^{\frac{\theta}{\theta-1}}. \tag{28}$$

A vast body of literature in climate macroeconomics utilizes DICE-type models to estimate the SCC in dollars per ton of CO_2. These studies highlight three main drivers of the shadow price of carbon: i) the discount rate, ii) the damage function, and iii) climate sensitivity to emissions and cumulative CO_2. Consequently, carbon prices can vary widely, from \$10 to \$1000 per ton (Traeger (2023)).

We begin by demonstrating that the elasticity of substitution between different capital stocks, which has not received much attention in the climate economics literature, can be a primary driver of the SCC (expressed in dollars per ton of CO_2) and of the shadow prices of natural capital. To this end, we contrast our main macro framework with a model that includes only energy as a natural capital input.

4.3.1 The Social Cost of Carbon under Various Specifications

In this part, we present the sensitivity of the SCC under our two model specifications to: i) climate damages β_m^h, ii) the climate transition parameter ζ_1, iii) the discount rate β, and ii) the elasticity of substitution (first nest) θ.[26] We will start by discussing the results of the sensitivity analysis to the first three parameters before turning to the elasticity of substitution, which has received less attention in the literature.

---

[25]The social planner problem and all equilibrium conditions are detailed in the appendix.

[26]While our empirical estimates for the elasticity of substitution between the two lower nests fall within the range reported in the literature, there is scarce literature available on the elasticities of substitution between natural capitals to validate our findings. Therefore, we conduct a sensitivity analysis regarding the elasticity of substitution (θ) between the first CES layer (i.e., capital, human capital, minerals, energy, forest ecosystem services, and cropland) to further explore this aspect.

Sensitivity of the Social Cost of Carbon to Climate Damages, Discount Rate, and Climate Dynamics. Our baseline calibration is depicted by the dashed line in figure 2. This results in a price of \$63 per tCO_2 for the main model specification including all natural capital, and \$56 per tCO_2 for the model with energy only. Comparing the model with natural capital to the one with only energy, we find that the SCC is approximately 12 percent higher when natural capital is accounted for in the production function compared to when it is not. This finding underscores the importance of including natural capital climate damages and highlights the undervaluation of the SCC in many DICE-style models. Additionally, uncertainty regarding the evolution of climate damages can significantly impact the optimal CO_2 price. We observe that the carbon price would double and quadruple in both models if damages were two and four times the baseline estimates, respectively. This result aligns with the specification of our damage functions and findings in previous literature.[27] Similarly, uncertainty over the discount rate is shown to have an important impact on the SCC, whereby the baseline value can range between \$25 per tCO_2 to about \$200 per tCO_2. This is well documented in the literature as well and heavily debated (e.g. Stern (2008) and Nordhaus (2008)). In contrast, the impacts of climate sensitivity in our analysis are relatively mild compared to the literature Folini, Friedl, Kübler, and Scheidegger (2024) for two reasons: i) temperature and cumulative emissions are calibrated to match the 2018 world values, which limits the influence of the climate transient parameter ζ_1 on SCC, and ii) our analysis primarily focuses on static dynamics where the transmission powers of ζ_1 are attenuated compared to its significant role in transitional dynamics.

---

[27]We acknowledge that tipping points, which would disrupt the linear impact of damages on the SCC, are not explicitly modeled here. However, incorporating tipping points would only reinforce our results.
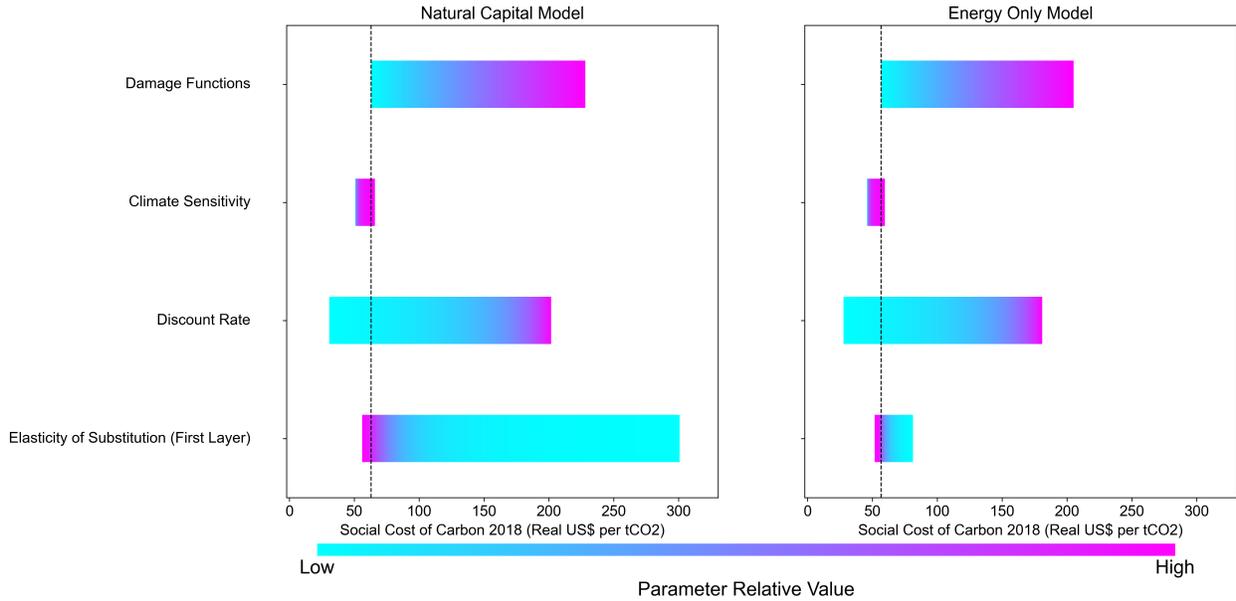
Figure 2: Social Cost of Carbon Sensitivity

Notes: This figure displays the SCC under two different model specifications across varying parameter ranges. Monte Carlo draws are performed at uniform intervals for each parameter, and SCC values are reported accordingly. The parameters are chosen as follows: $\beta_m^h \in$ (Baseline, $4 \times$ Baseline), $\theta \in (0.2, 3.5)$, $\beta \in (0.94, 0.99)$, and $\zeta_1 \in (0.1, 2)$. The color shades indicate the sensitivity of the SCC to changes in parameter values. For example, the SCC increases linearly with climate damages, whereas it shows a non-linear response to changes in the elasticity of substitution.

Sensitivity of the Social Cost of Carbon to the Elasticity of Substitution Between Production Factors. The significance of natural capital is underscored by the sensitivity analysis concerning the elasticity of substitution between production factors. We find that the SCC exhibits high sensitivity to the values of θ. When natural capital tends towards complementarity (i.e., lower degree of substitutability, $\theta \leq 1$), the SCC increases non-linearly to approximately 4.5 times compared to the baseline estimate of $\theta = 1.7$ (\$63 per tCO$_2$). Importantly, in the model without natural capital, the sensitivity of SCC to variations in the elasticity of substitution is mild compared to the main model with various types of natural capital (the SCC increases by only about 50 percent between the two extreme cases). This finding emphasizes two key points: i) the crucial role of including natural capital in macro-climate framework and policy analysis, ii) the necessity for further exploration of these elasticities considering regional and income heterogeneity, where some natural capitals may tend towards complementarity in certain regions (e.g., see table 30).

4.3.2 Production Factors' Shadow Prices under Various Specifications

We now turn our attention to the sensitivity of production factors' shadow prices to the value of the four parameters highlighted above. Consistent with the previous subsection, we will first discuss results related to parameters often considered in the literature, before moving to the elasticity of substitution between production factors.

Sensitivity of Shadow Prices to Climate Damages, Discount Rate, and Climate Dynamics. We observe that climate damages, the discount rate, and climate transient parameters only impact the shadow prices of fossil energy and its inputs—oil, gas, and coal—as shown in figure 11, figure 12, and figure 13. This is expected as all other shadow prices in our static exercise can only be impacted by the various components of the production function of the layer to which they belong. In the case of fossil energy and its components, however, the optimal price of carbon enters the formula for shadow prices. As the social cost of carbon grows, fossil inputs become undesirable for the social planner, and their respective shadow prices fall. The effect is thus only indirect, through the impact on the SCC discussed in the previous subsection. The reason is that we target specific levels of production for each type of production input to match the observed levels in 2018. Hence, even though the social planner would theoretically like to reduce the economy's reliance on fossil fuels, the static analysis does not allow it. This limitation will be lifted when we study transition dynamics, where both shadow prices, stocks, and flows will be allowed to move freely.

Sensitivity of Shadow Prices to the Elasticity of Substitution Between Production Factors. Figure 3 shows the sensitivity of shadow prices to the calibration of the elasticity of substitution between production factors. Focusing initially on the full model, it is evident that all natural capital shadow prices experience a substantial increase, each at least doubling compared to the baseline case with $\theta = 1.7$. The difficulty of substituting between different natural capitals, produced capital, and human capital becomes considerably more pronounced, resulting in upward pressure on the shadow prices of less abundant resources. This effect is even more pronounced in the model comprising solely energy. In that setup, the reduced substitutability is even more stringent, as there are only three inputs to the production function. This result also helps to explain the relatively low sensitivity of the SCC in the energy-only model. As inputs become less substitutable, the social planner has no choice but to continue relying on fossil inputs. Given the very high social value attached to these inputs, the SCC cannot increase as much as it would when including other types of natural capital.
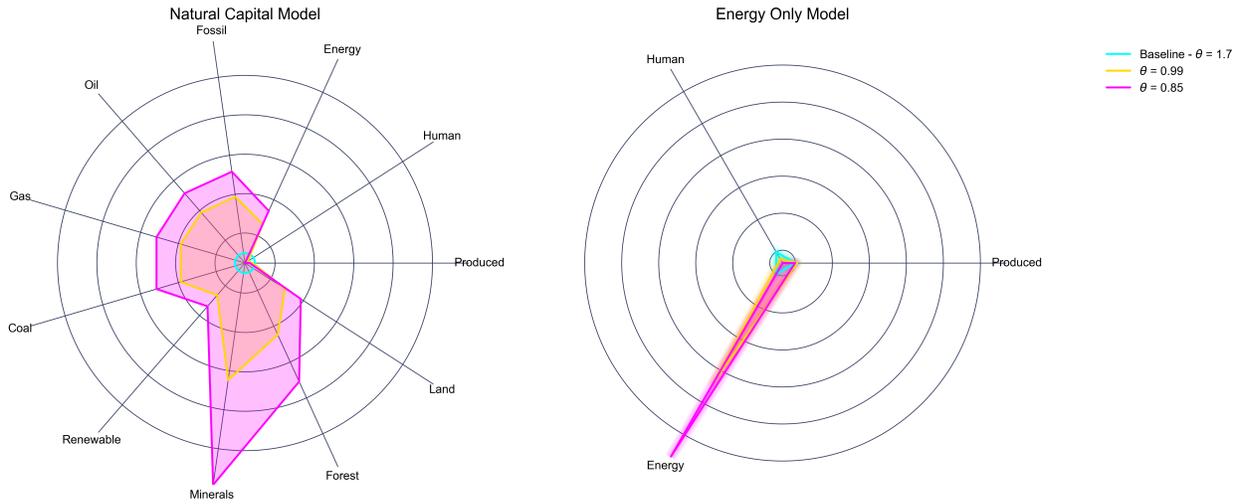
Figure 3: Shadow Prices Sensitivity To Elasticity of Substitution

Notes: This figure shows production factors' shadow prices under two different model specifications across three parameter values representing distinct scenarios: i) baseline, ii) Cobb-Douglas case with $\theta \approx 1$, iii) low substitution $\theta = 0.85$. The baseline case shadow prices are normalized to one and the center of the circle correspond the lowest shadow price value.

4.4 Long-run Dynamics of the SCC and Natural Capital

We now illustrate the evolution of the SCC and each natural capital over time. The economy is projected to grow at a 3 percent annual growth rate in human capital from 2018 to 2125.

Figure 4 shows the dynamics of aggregate output, temperature, and the SCC for both model specifications.
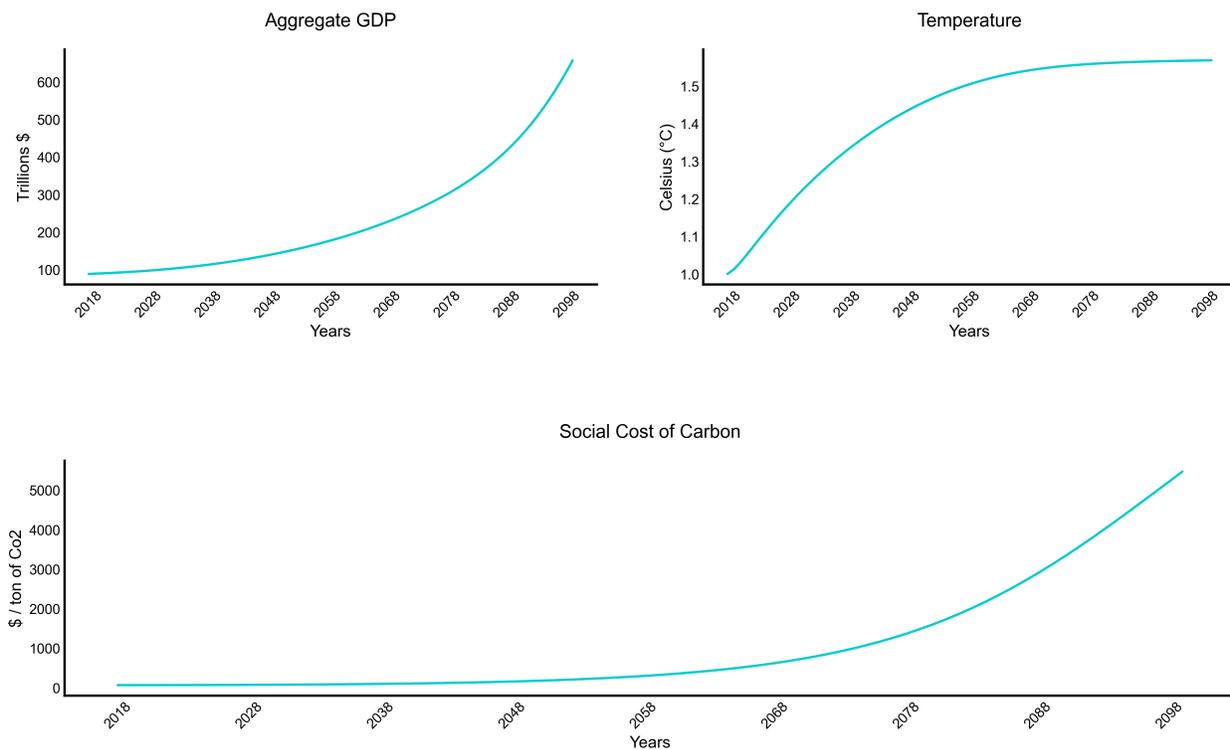
Figure 4: Long-Run Transition : Social Cost of Carbon

Notes: This figure illustrates the long-run transition over 82 years (up to 2100) with a 3 percent growth rate.

First, focusing on the main model specification with all types of natural capital, aggregate output rises with human capital. This rise implies an increase in the SCC to counteract the negative impacts of rising temperatures on production inputs. The increase in the SCC results in a gradual phasing out of fossil energy and promotes the use of renewable energy, which is CO_2-free, as illustrated in figure 5. The phasing out of fossil fuels is due to the decrease in all fossil fuel components: oil, gas, and coal (see figure 16).

The social planner by internalizing the impacts of the climate externality by taking into account the shadow price of CO_2 is able to keep temperature below 2^oC by 2100.
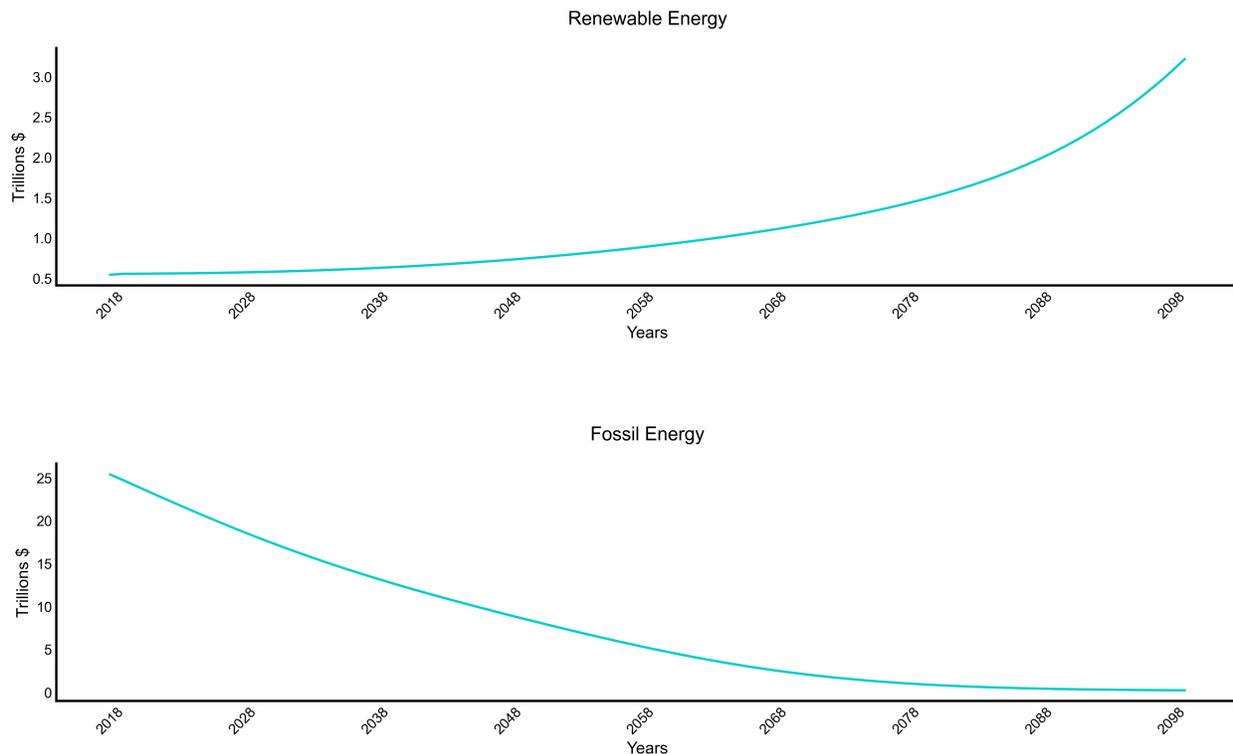
Figure 5: Long-Run Transition: Energy Components

Notes: This figure illustrates the long-run transition over 82 years (up to 2100) with a 3 percent growth rate.

A small initial dip in all types of natural capital as well as in produced capital (presented in figure 14 and figure 15) due to the substitution effect towards human capital is noticed. This effect, however, is temporary. As human capital becomes more efficient through exogenous growth, the need for other inputs is reduced. However, in the long run, the transition to clean energy and the improvement of ecosystems are still assured by the social planner.

4.5 The Role of Uncertainty

In this section we highlight the importance of accounting for uncertainty both from a policy design and modeling perspectives. We demonstrate how aggregate uncertainty in: i) TFP and temperature impacts the SCC in the presence of habit formation, which is crucial for optimal policy design, and ii) the discovery/investment rate impacts the SCC.

4.5.1 Uncertainty and Shadow Prices

Recent literature (e.g., Barnett, Brock, and Hansen (2021) and Benmir et al. (2020)) emphasizes that uncertainty is a crucial factor when assessing the optimal value of the carbon price. In particular, economic uncertainty can significantly impact the stochastic discount factor, a key element in the climate debate (Stern (2008) and Nordhaus (2008)). The stochastic discount factor is highly sensitive to utility function choices and time discounting. Benmir et al. (2020) argue that, while habit formation is essential for aligning macro models with both financial prices and macroeconomic aggregates, it also has important implications for the SCC. We thus contrast our results on the impact of uncertainty using versions of the model with and without habit formation à la Jaccard (2014).

In the following, we demonstrate how the theoretical mean of the SCC, as well as natural capital shadow costs, varies when accounting for uncertainty regarding productivity and temperature. We standardize both shocks to a 1 percent standard deviation[28] and compute the conditional mean of the shadow prices at the second order.

The results presented in table 9 illustrate how shadow prices responds to the inclusion of stochastic TFP. In the scenario without habit formation, when accounting for uncertainty around TFP, all natural capital shadow prices, as well as the carbon price, increase. These results are expressed as percentage deviations from the deterministic case under three elasticity of substitution scenarios.

---

[28]This corresponds to annual variations of 1 percent in final output and around 0.01°C in temperature.

Name	Variable	All Natural Capital			Only Energy		
		$\theta = 0.85$	$\theta = 0.99$	$\theta = 1.70$	$\theta = 0.85$	$\theta = 0.99$	$\theta = 1.70$
Shadow Cost of Emission	$E(V^{\mathrm{E}})$	0.04	0.03	0.13	0.02	0.01	0.06
		(3.27)	(3.26)	(3.91)	(3.03)	(3.19)	(3.93)
Shadow Cost of Energy	$E(\Psi^{\mathrm{E}})$	0.02	0.02	0.04	0.03	0.03	0.01
		(2.30)	(2.29)	(2.06)	(3.06)	(3.26)	(3.26)
Shadow Cost of Fossil	$E(\Psi^{\mathrm{FE}})$	0.01	0.02	-0.02	-	-	-
		(2.96)	(3.11)	(3.67)	-	-	-
Shadow Cost of Oil	$E(\Psi^{\mathrm{O}})$	0.01	0.02	-0.02	-	-	-
		(2.94)	(3.08)	(3.54)	-	-	-
Shadow Cost of Gas	$E(\Psi^{\mathrm{G}})$	0.01	0.02	-0.01	-	-	-
		(2.87)	(2.97)	(3.03)	-	-	-
Shadow Cost of Coal	$E(\Psi^{\mathrm{C}})$	0.01	0.01	-0.02	-	-	-
		(3.00)	(3.16)	(3.92)	-	-	-
Shadow Cost of Renewable Energy	$E(\Psi^{\mathrm{RE}})$	0.02	0.03	0.02	-	-	-
		(2.25)	(2.17)	(1.19)	-	-	-
Shadow Cost of Minerals	$E(\Psi^{\mathrm{M}})$	0.15	0.18	0.06	-	-	-
		(3.17)	(3.29)	(3.52)	-	-	-
Shadow Cost of Eco System Services	$E(\Psi^{\mathrm{FO}})$	-0.01	-0.01	-0.03	-	-	-
		(2.92)	(3.00)	(2.87)	-	-	-
Shadow Cost of Land	$E(\Psi^{\mathrm{L}})$	0.04	0.05	-0.01	-	-	-
		(2.79)	(2.92)	(3.29)	-	-	-

Table 9: Uncertainty cost of TFP shock for different θ values – percentage change with respect to deterministic case

Notes: This table displays the impact of TFP uncertainty on shadow prices under our two different model specifications and three cases for elasticity of substitution in the first layer. The third column corresponds to the estimated elasticity. The first column assumes an elasticity lower than unity, and the second one is an intermediate case. Results are reported as percentage deviations from the deterministic case. Standard deviations are reported in parentheses. E(X) refers to the expectation of the shadow price X.

The impact of the shock is entails a price increase with respect to the deterministic case. Specifically, in the case of the SCC, the price increase ranges from 0.02 to 0.13 percent. These effects are relatively mild and would not entail substantial policy implications. Similar orders of magnitude are observed with respect to shadow prices. Additionally, uncertainty impacts are slightly higher under the natural capital framework compared to its counterpart. This explains why uncertainty was not considered of first-order importance in early climate economics literature discussions on SCC drivers (e.g., Nordhaus and Moffat (2017) and Stern (2008)).

However, when incorporating habit formation in table 10, which enhances the model's predictive capacity by allowing it to match both financial and macroeconomic moments, the impact on all shadow prices is

magnified by a factor of 300 to 1700,[29] emphasizing the importance of accounting for uncertainty in optimal allocation analysis. In the case of the natural capital framework, the SCC prices increase to values ranging between 22 percent and 68 percent compared to the deterministic case. Furthermore, including natural capital versus excluding it can have serious policy implications. We find that SCC uncertainty impacts can be up to 4.7 times higher when accounting for natural capital, particularly under low elasticity of substitution.

Name	Variable	All Natural Capital			Only Energy		
		$\theta = 0.85$	$\theta = 0.99$	$\theta = 1.70$	$\theta = 0.85$	$\theta = 0.99$	$\theta = 1.70$
Shadow Cost of Emission	$E(V^{\mathrm{E}})$	68.04	22.12	39.67	14.39	15.62	31.22
		(68.66)	(45.14)	(26.73)	(41.39)	(41.05)	(33.35)
Shadow Cost of Energy	$E(\Psi^{\mathrm{E}})$	11.61	2.17	7.45	0.36	-0.51	-11.31
		(20.67)	(11.70)	(6.14)	(29.37)	(31.37)	(25.72)
Shadow Cost of Fossil	$E(\Psi^{\mathrm{FE}})$	-0.09	-3.11	-16.04	-	-	-
		(53.79)	(30.54)	(25.15)	-	-	-
Shadow Cost of Oil	$E(\Psi^{\mathrm{O}})$	0.13	-2.93	-15.78	-	-	-
		(53.07)	(30.10)	(24.03)	-	-	-
Shadow Cost of Gas	$E(\Psi^{\mathrm{G}})$	0.16	-2.80	-13.93	-	-	-
		(51.64)	(28.90)	(19.45)	-	-	-
Shadow Cost of Coal	$E(\Psi^{\mathrm{C}})$	-0.25	-3.27	-16.72	-	-	-
		(54.71)	(31.21)	(27.34)	-	-	-
Shadow Cost of Renewable Energy	$E(\Psi^{\mathrm{RE}})$	2.92	-0.32	-8.35	-	-	-
		(38.34)	(19.91)	(3.70)	-	-	-
Shadow Cost of Minerals	$E(\Psi^{\mathrm{M}})$	35.87	13.23	-35.91	-	-	-
		(47.55)	(29.92)	(31.96)	-	-	-
Shadow Cost of Eco System Services	$E(\Psi^{\mathrm{FO}})$	-4.24	-5.63	-9.63	-	-	-
		(58.54)	(31.27)	(18.37)	-	-	-
Shadow Cost of Land	$E(\Psi^{\mathrm{L}})$	5.59	0.13	-19.65	-	-	-
		(48.35)	(28.28)	(24.95)	-	-	-

Table 10: Uncertainty cost of TFP shock for different θ values – percentage change with respect to deterministic case (habits case)

Notes: This table displays the impact of TFP uncertainty on shadow prices under our two different model specifications with habit formation and three cases for elasticity of substitution in the first layer. The third column corresponds to the estimated elasticity. The first column assumes an elasticity lower than unity, and the second one is an intermediate case. Results are reported as percentage deviations from the deterministic case. Standard deviations are reported in parentheses. E(X) refers to the expectation of the shadow price X.

With respect to temperature, we find that the impacts on the SCC and the different shadow prices are negligible compared to the case of TFP, The reason is that these shocks only marginally impact the marginal utility of consumption, and thus the stochastic discount factor (see table 28). As a consequence, results are

[29]Taking an approximate ratio between the results in table 10 and table 9.

comparable when switching on habit formation (see table 29).

4.5.2 Uncertainty and Discoveries/Investment

Announcing a strong commitment to carbon pricing is likely to create anticipatory effects among agents. This could result in an initial uptick in the use of existing fossil energy resources, potentially leading to the unexpected discovery of additional oil, gas, or coal reserves. Understanding the implications of such sudden increases in fossil energy production on the Social Cost of Carbon (SCC) is critical for the effective decarbonization of the economy.

In our final exercise, we utilize the stationarized models to illustrate the impacts of uncertainty in discoveries and investments on the SCC.
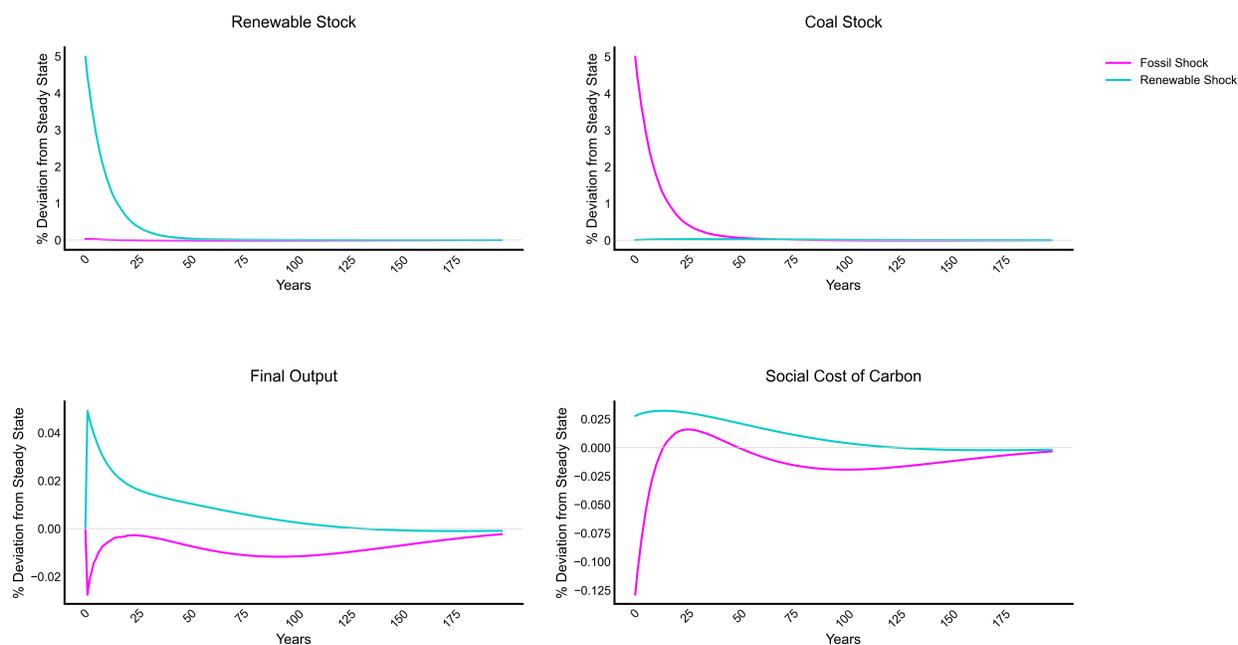
Figure 6: Impulse Response Function: Energy and Social Cost of Carbon

Notes: This figure displays the impulse responses of the fossil stock (coal), renewable stock, and the SCC to a shock in the intensity of gas discoveries and investment in renewables corresponding to a 5% increase in the stock of gas and renewables, respectively. The result holds for oil and gas too. The results are presented as a percentage deviation to the steady state, where the zero x-axis represents the steady state.

Figure 6 presents the impulse responses of the fossil stock (coal), the renewable stock, and the social cost of carbon (SCC) to a shock in the intensity of gas discoveries and investment in renewables. These shocks correspond to a 5% increase in the stock of gas and renewables, respectively. The results are shown

as deviations from the steady state. We compare two scenarios: (i) a shock to the discovery rate in the coal stock, and (ii) a shock to the investment rate in renewables.

Our results highlight the relative importance of renewable investment compared to potential fossil stock discoveries (coal). While policymakers might be concerned that new fossil discoveries could hinder progress toward a net-zero economy, our findings suggest that the economic impact of these discoveries is mild. Although their quantitative effects are small (with GDP decreasing by 0.03% for a 5% increase in fossil discoveries), they do result in reductions in both GDP and SCC. This outcome is driven by the high substitutability between natural capital stocks in the economy. Figure 17 further illustrates how a discovery shock decreases the shadow price of coal following an increase in coal availability, making it more abundant. At the same time, the shadow prices of other energy sources rise, ultimately leading to a decline in total output. In contrast, a positive investment shock in renewables significantly boosts final output, which, in turn, increases the SCC as a corrective mechanism to offset rising emissions.

In conclusion, in a first-best economy where a social planner internalizes the negative externalities of temperature damages, renewable investments are more welfare-enhancing as they increase output. In contrast, fossil fuel discoveries lead to welfare distortions, as reflected in lower output levels.

5   Conclusion

The rapid degradation of Earth's ecosystems has significant implications for economic production. In this paper, we demonstrated that incorporating natural capital dynamics and their interaction with climate dynamics in macroeconomic models is crucial for optimal allocation analysis. To calibrate our model, we used state-of-the-art climate econometric methods to estimate damage functions for each type of natural capital and provided new estimates of elasticity of substitution between various production inputs. With these estimates, we quantified the impact of including natural capital in a macroeconomic model featuring uncertainty.

Our findings indicate that the SCC is about 12 percent higher in the fully-fledged model compared to the baseline. Additionally, all shadow prices are highly sensitive to the elasticity of substitution in the final output production function and the calibration of damage functions. We also computed the mean of the shadow prices, conditional on the expectation of shocks to productivity and temperature. Accounting for the stochastic nature of productivity increases the SCC by 0.13 percent to 39 percent, depending on the inclusion of habit formation. However, accounting for a moderate risk of temperature variation does not

significantly impact shadow prices.

In conclusion, our study highlights the importance of considering natural capital and the role of uncertainty in macroeconomic models. Ignoring natural capital can lead to substantial underestimation of the SCC and other shadow prices, ultimately affecting policy decisions and long-term sustainability.

6 Bibliography

D. Acemoglu, P. Aghion, L. Bursztyn, and D. Hemous. The environment and directed technical change. *American Economic Review*, 102(1):131–66, 2012.

M. Barnett, W. Brock, and L. P. Hansen. Climate Change Uncertainty Spillover in the Macroeconomy. In *NBER Macroeconomics Annual 2021, volume 36*, NBER Chapters. National Bureau of Economic Research, Inc, November 2021. URL https://ideas.repec.org/h/nbr/nberch/14556.html.

A. I. Barreca. Climate change, humidity, and mortality in the united states. *Journal of Environmental Economics and Management*, 63(1):19–34, 2012.

B. Bastien-Olvera, M. Conte, X. Dong, T. Briceno, D. Batker, J. Emmerling, M. Tavoni, F. Granella, and F. Moore. Unequal climate impacts on global values of natural capital. *Nature*, 625(7996):722–727, 2024.

B. A. Bastien-Olvera and F. C. Moore. Use and non-use value of nature and the social cost of carbon. *Nature Sustainability*, 4(2):101–108, 2021.

G. Benmir, I. Jaccard, and G. Vermandel. Green asset pricing. Technical report, ECB Working Paper, 2020.

M. Burke and K. Emerick. Adaptation to climate change: Evidence from us agriculture. *American Economic Journal: Economic Policy*, 8(3):106–140, 2016.

M. Burke, S. M. Hsiang, and E. Miguel. Global non-linear effect of temperature on economic production. *Nature*, 527(7577):235–239, 2015.

T. Carleton, A. Jina, M. Delgado, M. Greenstone, T. Houser, S. Hsiang, A. Hultgren, R. E. Kopp, K. E. McCusker, I. Nath, et al. Valuing the global mortality consequences of climate change accounting for adaptation costs and benefits. *The Quarterly Journal of Economics*, 137(4):2037–2105, 2022.

I. Choi. Unit root tests for panel data. *Journal of international money and Finance*, 20(2):249–272, 2001.

V. Corbo. Second-Order Approximations for Estimating Production Functions. In *Annals of Economic and Social Measurement, Volume 5, number 1*, NBER Chapters, pages 65–73. National Bureau of Economic Research, Inc, May 1976. URL https://ideas.repec.org/h/nbr/nberch/10428.html.

M. Dell, B. F. Jones, and B. A. Olken. Temperature shocks and economic growth: Evidence from the last half century. *American Economic Journal: Macroeconomics*, 4(3):66–95, 2012.

O. Deschênes and M. Greenstone. The economic impacts of climate change: evidence from agricultural output and random fluctuations in weather. *American economic review*, 97(1):354–385, 2007.

O. Deschênes and M. Greenstone. Climate change, mortality, and adaptation: Evidence from annual fluctuations in weather in the us. *American Economic Journal: Applied Economics*, 3(4):152–185, 2011.

O. Deschênes, M. Greenstone, and J. Guryan. Climate change and birth weight. *American Economic Review*, 99(2):211–217, 2009.

S. Dietz and F. Venmans. Cumulative carbon emissions and economic policy: in search of general principles. *Journal of Environmental Economics and Management*, 96:108–129, 2019.

M. Drupp, M. Hänsel, E. Fenichel, M. Freeman, C. Gollier, B. Groom, G. Heal, P. Howard, A. Millner, F. Moore, et al. Accounting for the increasing benefits from scarce ecosystems. *Science*, 383(6687): 1062–1064, 2024.

M. A. Drupp and M. C. Hänsel. Relative prices and climate policy: how the scarcity of nonmarket goods drives policy evaluation. *American Economic Journal: Economic Policy*, 13(1):168–201, 2021.

M. S. Feldstein. Alternative methods of estimating a ces production function for britain. *Economica*, 34 (136):384–394, 1967.

D. Folini, A. Friedl, F. Kübler, and S. Scheidegger. The climate in climate economics. *Review of Economic Studies*, page rdae011, 2024.

J. Graff Zivin and M. E. Kahn. Industrial productivity in a hotter world: the aggregate implications of heterogeneous firm investment in air conditioning. Technical report, National Bureau of Economic Research, 2016.

J. Graff Zivin and M. Neidell. Temperature and the allocation of time: Implications for climate change. *Journal of Labor Economics*, 32(1):1–26, 2014.

R. L. Graham, M. G. Turner, and V. H. Dale. How increasing co2 and climate change affect forests. *BioScience*, 40(8):575–587, 1990.

A. Henningsen and G. Henningsen. On estimation of the ces production function—revisited. *Economics Letters*, 115(1):67–69, 2012. URL https://EconPapers.repec.org/RePEc:eee:ecolet:v:115:y:2012:i:1:p:67-69.

A. Hoff. The linear approximation of the ces function with n input variables. *Marine Resource Economics*, 19(3):295–306, 2004. ISSN 07381360, 23345985. URL http://www.jstor.org/stable/42629436.

S. Hsiang. Climate econometrics. *Annual Review of Resource Economics*, 8:43–75, 2016.

IPCC. Climate change and land: an ipcc special report on climate change, desertification, land degradation, sustainable land management, food security, and greenhouse gas fluxes in terrestrial ecosystems. *In press*, 2019.

I. Jaccard. Asset returns and labor supply in a production economy. *Journal of Money, Credit and Banking*, 46(5):889–919, 2014. ISSN 00222879, 15384616.

H. D. Jacoby, J. M. Reilly, J. R. McFarland, and S. Paltsev. Technology and technical change in the mit eppa model. *Energy Economics*, 28(5):610–631, 2006. ISSN 0140-9883. doi: https://doi.org/10.1016/j.eneco.2006.05.014. URL https://www.sciencedirect.com/science/article/pii/S0140988306000624. Modeling Technological Change in Climate Policy Analyses.

A. Jo. Substitution between clean and dirty energy with directed technical change. *Available at SSRN 4211251*, 2022.

A. Jo and A. Miftakhova. How constant is constant elasticity of substitution? endogenous substitution between clean and dirty energy. *Journal of Environmental Economics and Management*, 125:102982, 2024.

D. P. Kingma and J. Ba. Adam: A method for stochastic optimization, 2017. URL https://arxiv.org/abs/1412.6980.

J. Kmenta. On estimation of the ces production function. *International Economic Review*, 8(2):180–189, 1967. ISSN 00206598, 14682354. URL http://www.jstor.org/stable/2525600.

M. Kotz, A. Levermann, and L. Wenz. The economic commitment of climate change. *Nature*, 628(8008): 551–557, 2024.

E. Lagomarsino. Estimating elasticities of substitution with nested ces production functions: Where do we stand? *Energy Economics*, 88(C):S0140988320300918, 2020. URL https://EconPapers.repec.org/RePEc:eee:eneeco:v:88:y:2020:i:c:s0140988320300918.

G. Maddala and J. B. Kadane. Estimation of returns to scale and the elasticity of substitution. *Econometrica, Journal of the Econometric Society*, pages 419–423, 1967.

H. D. Matthews, N. P. Gillett, P. A. Stott, and K. Zickfeld. The proportionality of global warming to cumulative carbon emissions. *Nature*, 459(7248):829–832, 2009.

R. P. McDonald. A simple comprehensive model for the analysis of covariance structures: Some remarks on applications. *British Journal of Mathematical and Statistical Psychology*, 33(2):161–183, 1980.

R. G. Newell, B. C. Prest, and S. E. Sexton. The gdp-temperature relationship: implications for climate change damages. *Journal of Environmental Economics and Management*, 108:102445, 2021.

W. Nordhaus. A question of balance: Weighing the options on global warming policies. Yale university press. *New Haven, CT*, 2008.

W. D. Nordhaus. To slow or not to slow: the economics of the greenhouse effect. *Economic Journal*, 101 (407):920–937, 1991.

W. D. Nordhaus. Geography and macroeconomics: New data and new findings. *Proceedings of the National Academy of Sciences*, 103(10):3510–3517, 2006.

W. D. Nordhaus and A. Moffat. A survey of global impacts of climate change: replication, survey methods, and a statistical analysis. 2017.

W. D. Nordhaus and Z. Yang. A regional dynamic general-equilibrium model of alternative climate-change strategies. *American Economic Review*, pages 741–765, 1996.

C. Papageorgiou, M. Saam, and P. Schulte. Substitution between clean and dirty energy inputs: A macroeconomic perspective. *The Review of Economics and Statistics*, 99(2):pp. 281–290, 2017. ISSN 00346535, 15309142. URL https://www.jstor.org/stable/26616117.

H. Qian, L. Wu, and J. Fan. On estimation of deep nested ces production functions. *Available at SSRN 3247693*, 2018.

R. Schaeffer, A. S. Szklo, A. F. P. de Lucena, B. S. M. C. Borba, L. P. P. Nogueira, F. P. Fleming, A. Troccoli, M. Harrison, and M. S. Boulahya. Energy sector vulnerability to climate change: A review. *Energy*, 38 (1):1–12, 2012.

W. Schlenker and M. J. Roberts. Nonlinear temperature effects indicate severe damages to us crop yields under climate change. *Proceedings of the National Academy of sciences*, 106(37):15594–15598, 2009.

R. Seidl, D. Thom, M. Kautz, D. Martin-Benito, M. Peltoniemi, G. Vacchiano, J. Wild, D. Ascoli, M. Petr, J. Honkaniemi, et al. Forest disturbances under climate change. *Nature climate change*, 7(6):395–402, 2017.

E. Somanathan, R. Somanathan, A. Sudarshan, and M. Tewari. The impact of temperature on productivity and labor supply: Evidence from indian manufacturing. *Journal of Political Economy*, 129(6):1797–1827, 2021.

N. Stern. The economics of climate change. *American Economic Review*, 98(2):1–37, 2008.

T. Sterner and U. M. Persson. An even sterner review: Introducing relative prices into the discounting debate. *Review of environmental economics and policy*, 2008.

R. Tarsia. Heterogeneous effects of weather shocks on firm economic performance. *Available at SSRN 4672552*, 2023.

J. Thursby and C. Lovell. An investigation of the kmenta approximation to the ces function. *International Economic Review*, 19(2):363–77, 1978. URL https://EconPapers.repec.org/RePEc:ier:iecrev:v:19:y:1978:i:2:p:363-77.

C. P. Traeger. Ace—analytic climate economy. *American Economic Journal: Economic Policy*, 15(3):372–406, 2023.

F. Van der Ploeg and A. Rezai. Optimal carbon pricing in general equilibrium: Temperature caps and stranded assets in an extended annual dsge model. *Journal of Environmental Economics and Management*, 110:102522, 2021.

Appendix A   Data

A.1   Descriptive Statistics

	Statistics				
	Average	Std. Dev.	Min.	Max.	Obs.
First Layer Variables					
Y^T	63.21	197.79	0.1062	2045.61	2,184
Y^K	280.36	878.59	0.2077	8622.27	2,184
Y^{AL}	557.65	2066.65	0.3627	20302.21	2,184
Y^{FO}	6.56	20.03	0.0001	199.02	2,184
Y^L	12.91	44.99	0.0194	516.22	2,184
Y^M	3.32	14.02	1.86E-06	249.08	2,184
Y^E	22.66	75.64	8.82E-08	716.05	2,184
Second Layer Variables					
Y^E	109.97	429.31	0.03	6871.14	3,478
Y^{FE}	84.03	349.02	0.00	5035.82	3,478
Y^{RE}	25.93	94.04	0.00	1835.32	3,478
Third Layer Variables					
Y^G	10.32	22.58	0.000025	161.98	1,152
Y^C	7.38	24.64	0.00005	220.34	1,152

Note: The first layer variables are expressed in 10 Billion Current 2018 USD, the second and third layer variables are expressed in terawatt hours.

Table 11: Summary Statistics: CES Estimates Data

	Statistics				
	Average	Std. Dev.	Min.	Max.	Obs.
Total Cropland	40.71	3.69	29.90	50.32	1,728
Forest Ecosystem	23.34	2.37	14.01	28.32	1,704
Minerals	21.35	3.19	11.94	28.54	1,368
Coal Electricity	2.86	2.32	-4.61	8.46	1,212
Gas Electricity	2.64	1.92	-4.61	7.29	1,548
Oil Electricity	1.39	1.98	-6.21	5.52	1,523
Fossil Fuel Electricity	3.75	1.72	-4.61	8.52	1,606
Renewable Electricity	2.29	2.21	-5.52	7.51	1,616
Energy	27.02	1.43	23.89	31.28	1,728
Temperature	14.85	8.26	-4.89	28.98	1,728
Precipitation	1072.72	793.83	6.11	4226.89	1,728

Note: All values except temperature and precipitation are expressed in logarithmic values.

Table 12: Summary Statistics: Climate Damages Estimates Data

(a) Cropland

(b) Forest Ecosystem

(c) Minerals

(d) Aggregate Energy
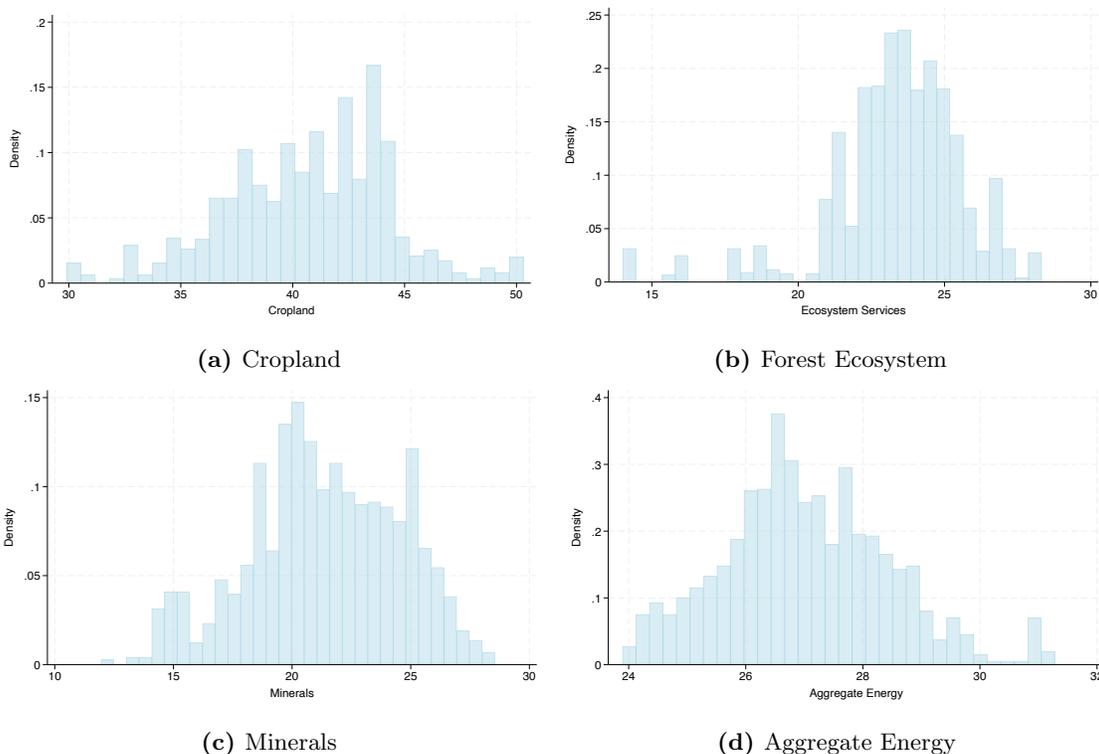
Figure 7: Density distributions for the variables in layer one.
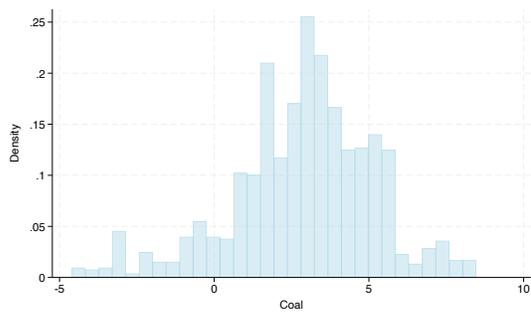
(a) Coal
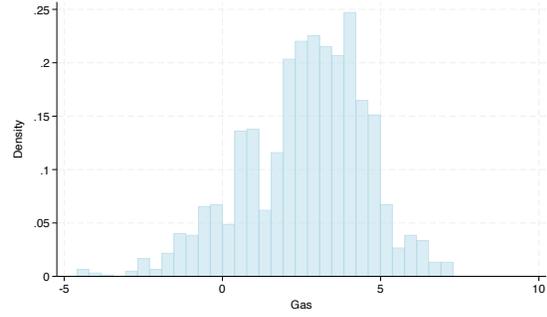
(b) Gas
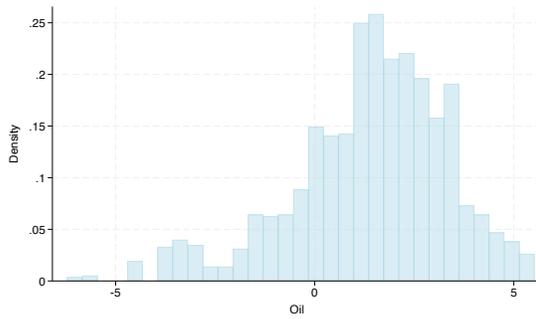
(c) Oil
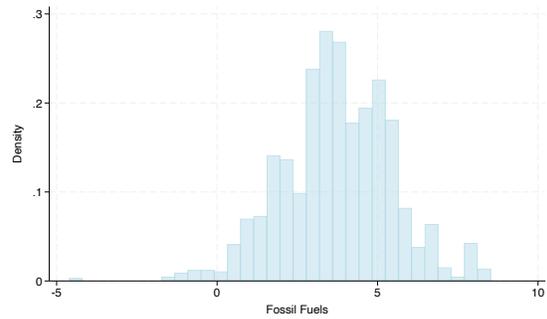
(d) Fossil fuell
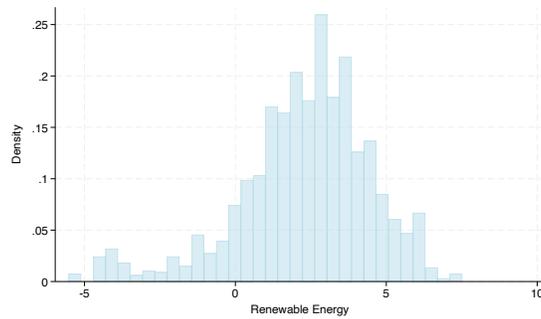
(e) Renewable energy

Figure 8: Density distributions for the variables in layers two and three.
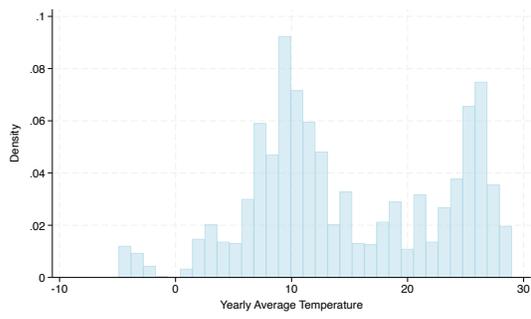
(a) Temperature
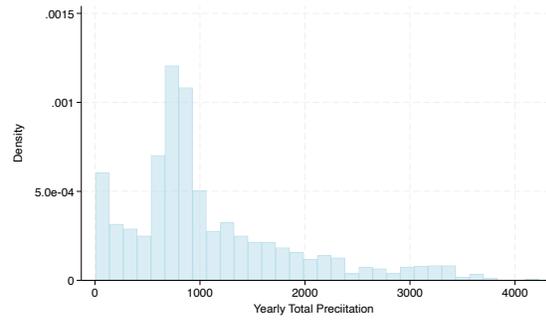
(b) Precipitation

Figure 9: Density distributions for the climate variables

Appendix B   CES Estimation Methods

B.0.1   Adam: A Stochastic Gradient Descent Method

Adam is a stochastic gradient descent (SGD) algorithm variant introduced by Kingma and Ba (2017). It is implemented using TensorFlow, a popular machine learning library.[30] While most of the literature relies on linear, non-linear, or indirect econometric approaches to estimate CES elasticities, Qian et al. (2018) employ machine learning methods for CES parameter estimation, specifically using Adadelta, another widely used SGD method. This work is the closest to our proposed estimation using Adam.

To respect the bounds of the parameters, constrained gradient descent requires a projection step to ensure that the parameters fall within the feasible set. However, this can be computationally expensive and face convergence issues, proving to be particularly challenging for the distribution and the elasticity of substitution parameters. Unlike SQP, we cannot introduce explicit constraints and as such, following McDonald (1980), we reparameterize the elasticity and each of the k distribution parameters as follows:

$$\rho = e^\lambda - 1 \tag{29}$$

$$\theta_k = \frac{1}{1 + e^{-\mu_k}} \tag{30}$$

This removes the need to explicitly constrain λ and μ_j while ensuring that $\rho \in (-1, \infty)$ and $\theta_k \in [0, 1]$. Ultimately, the objective of the problem is to minimize the sum of squared residuals (SSR) shown below where $Y_{i,t}^k$ denotes the inputs, γ is an efficiency parameter and f represents a production function, which in our case is a CES production function.

$$\min_{\gamma, \lambda, \mu} SSR_{i,t} = \min_{\gamma, \lambda, \mu} \sum_{t=1}^{T} (Y_{i,t} - f(\gamma, Y_{i,t}^k, \lambda, \mu_k))^2 \tag{31}$$

We use Adam to find the parameters that minimize SSR by updating them as shown below where t denotes the timestep in the optimization procedure and θ denotes the parameters. Adam differs from regular SGD since it computes adaptive learning rates for the parameters and updates these rates by computing two exponentially decaying averages of the first and second moments of past gradients. In doing so, it combines the features of Adadelta and AdaGrad methods [31]. Here, we provide a brief exposition of the algorithm (refer to Kingma and Ba (2017) for more details):

---

[30]Adam belongs to a broader class of adaptive learning rate algorithms, which includes AdaGrad, RMSProp, and Adadelta.
[31]See **?** for an overview of different SGD methods.

1. Initialise m_0 and v_0, the first and second moment respectively as a vector of zeros. Set the step-size/learning rate δ.

2. Derive gradients for a given parameter given by $g_t = \nabla_\theta r_t(\theta_{t-1})$ where r_t is the objective function as defined above.

3. Update the first (biased) moment as $m_t = \beta_1 \cdot m_{t-1} + (1 - \beta_1)g_t$ where β_1 is an exponential decay rate set at default 0.9.

4. Update the second (biased) moment as $v_t = \beta_2 \cdot v_{t-1} + (1 - \beta_2)g_t^2$ where β_2 is another exponential decay rate set at default 0.99.

5. Compute the bias-corrected versions of the first and second raw moment estimates as $\hat{m}_t = \frac{m_t}{(1 - \beta_1^t)}$ and $\hat{v}_t = \frac{v_t}{(1 - \beta_2^t)}$ respectively. This is to correct the moments' bias toward zero given their initialisation.

6. Update the parameters as $\theta_t = \theta_{t-1} - \delta \frac{\hat{m}_t}{\sqrt{\hat{v}_t} + \epsilon}$ where $\epsilon = 10^{-8}$ to prevent division by zero.

As discussed in Qian et al. (2018), the benefits of using machine learning tools such as TensorFlow is that it uses automatic differentiation to calculate the gradients of complex objective functions.

Appendix C   CES Empirical Estimations

	Estimation Method	
	NLS Fixed υ	NLS
θ_{KL}	0.5370	0.6715
θ_{FO}	0.0701	0.0000
θ_{L}	0.1481	0.0872
θ_{M}	0.0467	0.0109
θ_{E}	0.1980	0.2305
ρ_Y	-0.6112	-0.6067
g_Y	0.4023	0.3610
υ_Y	1.0000	0.9577
$\theta = \frac{1}{1+\rho_Y}$	2.5720	2.5426
Observations	2,184	2,184
MSE	0.0976	0.0935

Table 13: First Layer CES Estimates with Composite Production

	Second Layer Kmenta-Approximation OLS Results	
	Coefficient	[95% Conf. Interval]
$\ln(Y^{FE})$	0.4125***	[0.3954, 0.4296]
	(0.0087)	
$\ln(Y^{RE})$	0.4001***	[0.3850, 0.4153]
	(0.0077)	
$(\ln(Y^{FE}) - \ln(Y^{RE}))^2$	0.0424***	[0.0399, 0.0449]
	(0.0424)	
Cons.	1.3942***	[1.3380, 1.4503]
	(0.0286)	
R^2	0.9961	
N	2,911	

Table 14: Second Layer Regression Results

First Layer Elasticity of Substitution by Sample Size
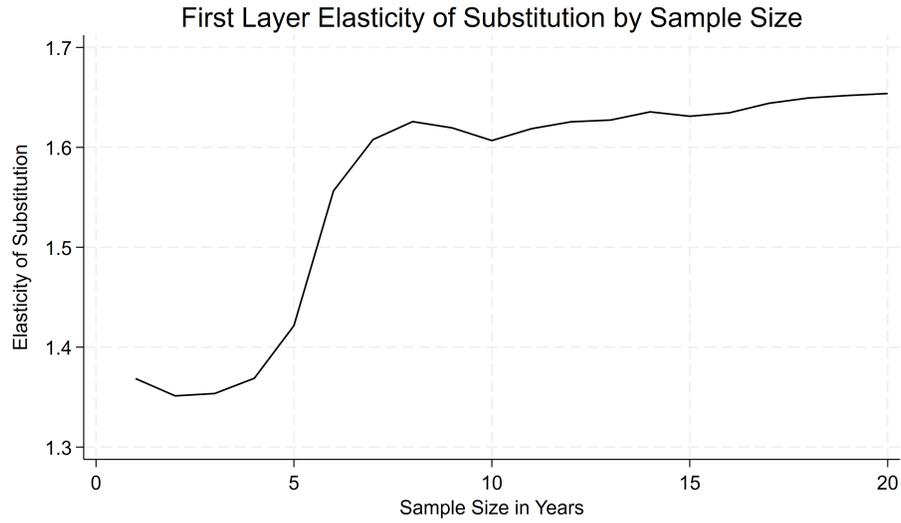
Figure 10: Evolution of Elasticity of Substitution by Sample Size

Notes: The sample size decreases as we move along the year dimension. Specifically, a sample size of 1 corresponds to the year 1995, a sample size of 2 represents the years 1995–1996, and a sample size of 20 encompasses the years 1995–2014.

	Third Layer Kmenta-Approximation OLS Results	
	Coefficient	[95% Conf. Interval]
$\ln(Y^{\mathrm{C}})$	0.2080***	[0.1469, 0.2691]
	(0.0312)	
$\ln(Y^{\mathrm{G}})$	0.2069***	[0.1501, 0.2637]
	(0.0289)	
$(\ln(Y^{\mathrm{C}}) - \ln(Y^{\mathrm{G}}))^2$	0.0112***	[0.0047, 0.0177]
	(0.0033)	
Cons.	3.9551***	[3.8886, 4.0215]
	(0.0339)	
R^2	0.9714	
N	1,152	

Table 15: Third Layer Regression Results

57

Appendix D   Climate Damages Regression Tables

	(1) Produced Capital	(2) Produced Capital	(3) Produced Capital	(4) Produced Capital	(5) Produced Capital	(6) Produced Capital
T	-0.040*** (0.0098)	-0.044*** (0.0096)	-0.030** (0.0084)	-0.13** (0.038)	-0.11*** (0.029)	-0.095*** (0.026)
P	-0.000025 (0.000024)	-0.000010 (0.000022)	0.000014 (0.000022)	-0.0000063 (0.000090)	-0.0000091 (0.000099)	0.000034 (0.000086)
$(\ell 1)T$		-0.035*** (0.0067)	-0.040*** (0.0088)		-0.096*** (0.025)	-0.088*** (0.023)
$(\ell 2)T$			-0.036*** (0.0086)			-0.051** (0.014)
T^2				0.0045** (0.0017)	0.0034* (0.0015)	0.0029* (0.0012)
P^2				3.5e-09 (0.000000016)	3.8e-09 (0.000000020)	-1.3e-09 (0.000000019)
$(\ell 1)T^2$					0.0031** (0.0011)	0.0028** (0.0011)
$(\ell 2)T^2$						0.00069*** (0.00019)
Country FE	Yes	Yes	Yes	Yes	Yes	Yes
Year FE	Yes	Yes	Yes	Yes	Yes	Yes
R^2	0.99	0.99	0.99	0.99	0.99	0.99
N	1728	1656	1584	1728	1656	1512

Standard errors in parentheses
* $p < 0.10$, ** $p < 0.05$, *** $p < 0.01$

Table 16: Point estimates and standard errors from the regressions of weather variables on produced capital. Results from different specifications with country and year FE, standard errors clustered at the regional level as identified by the World Bank.

	(1) Cropland	(2) Cropland	(3) Cropland	(4) Cropland	(5) Cropland	(6) Cropland
T	-0.034*** (0.0092)	-0.047*** (0.0087)	-0.015 (0.012)	-0.19** (0.064)	-0.16*** (0.042)	-0.10** (0.029)
P	0.000035 (0.000070)	0.000037 (0.000068)	0.000085 (0.000060)	-0.000060 (0.000080)	-0.000079 (0.000069)	-0.0000080 (0.000085)
$(\ell 1)T$		-0.039*** (0.0082)	-0.051*** (0.0081)		-0.12** (0.042)	-0.100** (0.040)
$(\ell 2)T$			-0.047*** (0.010)			-0.075*** (0.015)
T^2				0.0075** (0.0022)	0.0057*** (0.0014)	0.0041*** (0.00066)
P^2				0.000000037 (0.000000024)	0.000000036 (0.000000021)	0.000000029 (0.000000024)
$(\ell 1)T^2$					0.0043** (0.0017)	0.0035* (0.0016)
$(\ell 2)T^2$						0.0012** (0.00037)
Country FE	Yes	Yes	Yes	Yes	Yes	Yes
Year FE	Yes	Yes	Yes	Yes	Yes	Yes
R^2	1.00	1.00	1.00	1.00	1.00	1.00
N	1728	1656	1584	1728	1656	1512

Standard errors in parentheses
* $p < 0.10$, ** $p < 0.05$, *** $p < 0.01$

Table 17: Point estimates and standard errors from the regressions of weather variables on cropland. Results from different specifications with country and year FE, standard errors clustered at the regional level as identified by the World Bank.

	(1) ΔCoal	(2) ΔCoal	(3) ΔCoal	(4) ΔCoal	(5) ΔCoal	(6) Δ Coal
ΔT	-0.013 (0.013)	-0.0099 (0.020)	-0.0037 (0.020)	-0.039* (0.020)	-0.054 (0.035)	-0.053 (0.036)
$(\ell 1)\Delta T$		0.0096 (0.017)	0.021 (0.018)		-0.029 (0.027)	-0.035 (0.039)
$(\ell 2)\Delta T$			0.014** (0.0041)			-0.010 (0.017)
ΔP	-0.00010* (0.000046)	-0.00010* (0.000045)	-0.00011** (0.000035)	-0.00025** (0.000069)	-0.00024*** (0.000062)	-0.00023*** (0.000060)
ΔT^2				0.0013 (0.00085)	0.0022 (0.0013)	0.0025 (0.0015)
$(\ell 1)\Delta T^2$					0.0020 (0.0011)	0.0029 (0.0017)
$(\ell 2)\Delta T^2$						0.0013 (0.00086)
ΔP^2				0.000000046* (0.000000020)	0.000000042* (0.000000018)	0.000000035 (0.000000018)
Country FE	Yes	Yes	Yes	Yes	Yes	Yes
Year FE	Yes	Yes	Yes	Yes	Yes	Yes
R^2	0.13	0.14	0.14	0.13	0.15	0.15
N	1155	1111	1067	1155	1111	1067

Standard errors in parentheses
* $p < 0.10$, ** $p < 0.05$, *** $p < 0.01$

Table 18: Point estimates and standard errors from the regressions of weather variables on coal. Results from different specifications in first difference with country and year FE, standard errors clustered at the regional level as identified by the World Bank.

	(1) Gas	(2) Gas	(3) Gas	(4) Gas	(5) Gas	(6) Gas
T	-0.098*** (0.025)	-0.100** (0.028)	-0.084** (0.029)	-0.36** (0.098)	-0.33*** (0.084)	-0.31*** (0.074)
P	-0.00035*** (0.000057)	-0.00034*** (0.000076)	-0.00026** (0.000089)	-0.00037* (0.00018)	-0.00032 (0.00019)	-0.00015 (0.00015)
$(\ell 1)T$		-0.083*** (0.020)	-0.088*** (0.023)		-0.23*** (0.054)	-0.22*** (0.048)
$(\ell 2)T$			-0.098*** (0.017)			-0.11*** (0.026)
T^2				0.013** (0.0041)	0.011** (0.0034)	0.012*** (0.0029)
P^2				0.000000028 (0.000000044)	6.6e-09 (0.000000043)	-3.6e-09 (0.000000037)
$(\ell 1)T^2$					0.0074** (0.0024)	0.0071*** (0.0019)
$(\ell 2)T^2$						0.0016** (0.00044)
Country FE	Yes	Yes	Yes	Yes	Yes	Yes
Year FE	Yes	Yes	Yes	Yes	Yes	Yes
R^2	0.91	0.91	0.92	0.91	0.92	0.93
N	1548	1500	1452	1548	1500	1403

Standard errors in parentheses
* $p < 0.10$, ** $p < 0.05$, *** $p < 0.01$

Table 19: Point estimates and standard errors from the regressions of weather variables on gas. Results from different specifications with country and year FE, standard errors clustered at the regional level as identified by the World Bank.

	(1) Oil	(2) Oil	(3) Oil	(4) Oil	(5) Oil	(6) Oil
T	-0.048 (0.039)	-0.060 (0.038)	-0.041 (0.048)	-0.15 (0.12)	-0.13 (0.094)	-0.11 (0.088)
P	-0.00032 (0.00017)	-0.00033 (0.00018)	-0.00035* (0.00017)	-0.00051 (0.00034)	-0.00060 (0.00039)	-0.00056 (0.00034)
$(\ell 1)T$		-0.0063 (0.052)	-0.011 (0.051)		-0.11 (0.082)	-0.12 (0.073)
$(\ell 2)T$			0.031 (0.032)			0.057 (0.057)
T^2				0.0050 (0.0058)	0.0037 (0.0046)	0.0039 (0.0046)
P^2				0.000000061 (0.000000057)	0.000000074 (0.000000064)	0.000000053 (0.000000054)
$(\ell 1)T^2$					0.0051 (0.0049)	0.0063 (0.0047)
$(\ell 2)T^2$						-0.00098 (0.0014)
Country FE	Yes	Yes	Yes	Yes	Yes	Yes
Year FE	Yes	Yes	Yes	Yes	Yes	Yes
R^2	0.89	0.89	0.89	0.89	0.89	0.90
N	1523	1473	1423	1523	1473	1373

Standard errors in parentheses
* $p < 0.10$, ** $p < 0.05$, *** $p < 0.01$

Table 20: Point estimates and standard errors from the regressions of weather variables on oil. Results from different specifications with country and year FE, standard errors clustered at the regional level as identified by the World Bank.

	(1) Fossil Fuel	(2) Fossil Fuel	(3) Fossil Fuel	(4) Fossil Fuel	(5) Fossil Fuel	(6) Fossil Fuel
T	-0.080*** (0.019)	-0.084*** (0.018)	-0.063** (0.020)	-0.33*** (0.086)	-0.28*** (0.067)	-0.25*** (0.062)
P	-0.00016* (0.000070)	-0.00013* (0.000068)	-0.000091 (0.000080)	-0.00033** (0.00013)	-0.00035** (0.00012)	-0.00029* (0.00014)
$(\ell 1)T$		-0.054** (0.016)	-0.057** (0.019)		-0.21*** (0.045)	-0.19*** (0.041)
$(\ell 2)T$			-0.039** (0.015)			-0.041 (0.024)
T^2				0.012*** (0.0025)	0.0095*** (0.0019)	0.0090*** (0.0018)
P^2				0.000000070 (0.000000037)	0.000000068 (0.000000035)	0.000000058 (0.000000037)
$(\ell 1)T^2$					0.0075*** (0.0010)	0.0072*** (0.0011)
$(\ell 2)T^2$						0.00057 (0.00040)
Country FE	Yes	Yes	Yes	Yes	Yes	Yes
Year FE	Yes	Yes	Yes	Yes	Yes	Yes
R^2	0.97	0.97	0.97	0.97	0.97	0.97
N	1606	1555	1504	1606	1555	1453

Standard errors in parentheses
* $p < 0.10$, ** $p < 0.05$, *** $p < 0.01$

Table 21: Point estimates and standard errors from the regressions of weather variables on fossil fuel. Results from different specifications with country and year FE, standard errors clustered at the regional level as identified by the World Bank.

	(1) Δ Agg. Energy	(2) Δ Agg. Energy	(3) Δ Agg. Energy	(4) Δ Agg. Energy	(5) Δ Agg. Energy	(6) Δ Agg. Energy
ΔT	-0.014*** (0.0016)	-0.015*** (0.0027)	-0.016*** (0.0035)	-0.013*** (0.0025)	-0.016*** (0.0027)	-0.017*** (0.0030)
$(\ell 1)\Delta T$		-0.0032 (0.0017)	-0.0056 (0.0034)		0.0024 (0.0029)	-0.0012 (0.0032)
$(\ell 2)\Delta T$			-0.0013 (0.0024)			-0.0028 (0.0023)
ΔP	0.0000023 (0.000012)	0.0000017 (0.000012)	0.0000046 (0.000013)	0.000011 (0.000028)	0.0000093 (0.000031)	0.000018 (0.000029)
ΔT^2				-0.0000063 (0.00018)	0.000041 (0.00019)	0.00010 (0.00019)
$(\ell 1)\Delta T^2$					-0.00025** (0.00010)	-0.00020 (0.00014)
$(\ell 2)\Delta T^2$						0.000063 (0.000097)
ΔP^2				-2.4e-09 (6.6e-09)	-1.5e-09 (7.0e-09)	-3.1e-09 (5.9e-09)
Country FE	Yes	Yes	Yes	Yes	Yes	Yes
Year FE	Yes	Yes	Yes	Yes	Yes	Yes
R^2	0.24	0.25	0.26	0.24	0.25	0.26
N	1656	1584	1512	1656	1584	1512

Standard errors in parentheses
* $p < 0.10$, ** $p < 0.05$, *** $p < 0.01$

Table 22: Point estimates and standard errors from the regressions of weather variables on energy. Results from different specifications in first difference with country and year FE, standard errors clustered at the regional level as identified by the World Bank.

	(1) Ren. Energy	(2) Ren. Energy	(3) Ren. Energy	(4) Ren. Energy	(5) Ren. Energy	(6) Ren. Energy
T	-0.036 (0.022)	-0.028 (0.021)	-0.062** (0.020)	-0.0071 (0.064)	-0.027 (0.052)	-0.077 (0.058)
P	0.00024 (0.00013)	0.00027* (0.00012)	0.00022** (0.000082)	0.00062** (0.00022)	0.00065** (0.00019)	0.00044*** (0.00011)
$(\ell 1)T$		-0.033 (0.018)	-0.029 (0.018)		0.033 (0.061)	-0.0090 (0.057)
$(\ell 2)T$			-0.045 (0.024)			-0.044 (0.029)
T^2				-0.0012 (0.0022)	0.000093 (0.0017)	0.00087 (0.0022)
P^2				-0.000000097* (0.000000047)	-0.000000093* (0.000000040)	-0.000000057* (0.000000026)
$(\ell 1)T^2$					-0.0035 (0.0023)	-0.0029 (0.0022)
$(\ell 2)T^2$						-0.0000042 (0.00078)
Country FE	Yes	Yes	Yes	Yes	Yes	Yes
Year FE	Yes	Yes	Yes	Yes	Yes	Yes
R^2	0.96	0.96	0.96	0.96	0.96	0.96
N	1616	1549	1483	1616	1549	1416

Standard errors in parentheses
* $p < 0.10$, ** $p < 0.05$, *** $p < 0.01$

Table 23: Point estimates and standard errors from the regressions of weather variables on renewable energy. Results from different specifications with country and year FE, standard errors clustered at the regional level as identified by the World Bank.

	(1) Forest Eco.	(2) Forest Eco.	(3) Forest Eco.	(4) Forest Eco.	(5) Forest Eco.	(6) Forest Eco.
T	-0.0059 (0.0047)	-0.0087*** (0.0023)	-0.011** (0.0036)	-0.0098 (0.033)	-0.0087 (0.025)	-0.011 (0.024)
P	-0.0000022 (0.000020)	-0.0000084 (0.000021)	-0.000012 (0.000015)	0.000018 (0.000067)	0.000020 (0.000075)	-0.0000092 (0.000071)
$(\ell1)T$		-0.0087 (0.0047)	-0.011** (0.0038)		-0.014 (0.024)	-0.018 (0.023)
$(\ell2)T$			-0.0078 (0.0070)			-0.012 (0.010)
T^2				0.00020 (0.0018)	0.000022 (0.0013)	-0.000083 (0.0011)
P^2				-4.8e-09 (0.000000014)	-7.2e-09 (0.000000019)	2.3e-09 (0.000000017)
$(\ell1)T^2$					0.00023 (0.0012)	0.00021 (0.0011)
$(\ell2)T^2$						-0.000013 (0.00031)
Country FE	Yes	Yes	Yes	Yes	Yes	Yes
Year FE	Yes	Yes	Yes	Yes	Yes	Yes
R^2	1.00	1.00	1.00	1.00	1.00	1.00
N	1704	1633	1562	1704	1633	1491

Standard errors in parentheses
* $p < 0.10$, ** $p < 0.05$, *** $p < 0.01$

Table 24: Point estimates and standard errors from the regressions of weather variables on forest ecosystem. Results from different specifications with country and year FE, standard errors clustered at the regional level as identified by the World Bank.

	(1) Minerals	(2) Minerals	(3) Minerals	(4) Minerals	(5) Minerals	(6) Minerals
T	-0.075*** (0.016)	-0.064*** (0.012)	-0.027 (0.017)	-0.33** (0.11)	-0.25** (0.080)	-0.19* (0.083)
P	0.00013 (0.00012)	0.00012 (0.00011)	0.00014 (0.00013)	0.00073 (0.00052)	0.00055 (0.00055)	0.00045 (0.00081)
$(\ell1)T$		-0.095** (0.028)	-0.082** (0.026)		-0.32*** (0.072)	-0.28** (0.080)
$(\ell2)T$			-0.16*** (0.027)			-0.20** (0.062)
T^2				0.013** (0.0038)	0.0097** (0.0032)	0.0088** (0.0034)
P^2				-0.00000012 (0.00000010)	-0.000000096 (0.00000011)	-0.000000076 (0.00000015)
$(\ell1)T^2$					0.011** (0.0032)	0.011** (0.0040)
$(\ell2)T^2$						0.0027 (0.0015)
Country FE	Yes	Yes	Yes	Yes	Yes	Yes
Year FE	Yes	Yes	Yes	Yes	Yes	Yes
R^2	0.92	0.93	0.93	0.92	0.93	0.93
N	1368	1311	1254	1368	1311	1197

Standard errors in parentheses
* $p < 0.10$, ** $p < 0.05$, *** $p < 0.01$

Table 25: Point estimates and standard errors from the regressions of weather variables on minerals. Results from different specifications with country and year FE, standard errors clustered at the regional level as identified by the World Bank.

Appendix E   Model Results

E.1   Calibration and Moments Matching

Name	Variable	Value	Sensitivity
Climate Parameters			
Climate Transient Parameters 1	ϕ_1	0.5	$\in (0.1, 2)$
Climate Transient Parameters 2	ϕ_2	0.61	-
produced and Natural Capital Damages	β_m^h	refer to estimation	$\in (2 * \beta_m^h, 4 * \beta_m^h)$
Human Capital Damages	β_1^{AL}	- 0.02	$\in (2 * \beta_1^{AL}, 4 * \beta_1^{AL})$
Emission Intensity	ϕ_E	0.0014	-
Persistence of Temperature Shock	ρ_T	0.90	-
Temperature Shock Standard Deviation	σ_T	0.01	-
Macro Parameters			
Time preference	β	0.96	$\in (0.94, 0.99)$
Risk aversion	σ^H	2	-
Economy Growth Rate	γ^Γ	3%	-
Habits adjustment level	γ^H	0.975	-
Habits level	m	0.9	-
Labour hours	$\bar{L}$	1/3	-
Productivity of labour	A	$2.222e^3$	-
GDP scale	γ_Y	2.4	-
Energy scale	γ_E	1	-
Fossil Energy scale	γ_F	3	-
Inputs weights	θ_k	refer to estimation	-
Elasticity of Substitution First Layer	θ	refer to estimation	$\in (0.2, 3.5)$
Fossil Fuel Weight	σ_{FE}	refer to estimation	-
Renewable Energy Weight	σ_{RE}	refer to estimation	-
Elasticity of Substitution Second Layer	σ	refer to estimation	-
Elasticity of Substitution Third Layer	ϵ	refer to estimation	-
Oil, Gas, Coal Weights	ϵ_i	refer to estimation	-
Persistence of TFP Shock	ρ_A	0.90	-
Temperature Shock Standard Deviation	σ_A	0.01	-
Persistence of Discovery/Investment Shock	ρ_{D_i}	0.90	-
Temperature Shock Standard Deviation	σ_{D_i}	0.01	-

Table 26: Calibration

Variable	Label	Target	Source
Cumulative Emission (World, Trillion tCO2)	X	1.63	Ourworldindata
Yearly Emission Flow (World, GtCO2)	E	36.7	Ourworldindata
Temperature in Celcius	T	1.00	NOAA
World GDP in Trillion $	Y^T	86.5	WB Database
Produced Capital Stock in Trillion $	Y^K	358.4	WB Database
Human Capital Stock in Trillion $	Y^{AL}	727.2	WB Database
Renewable Energy Stock in Trillion $	Y^{RE}	0.5	Authors Calculation
Coal Stock in Trillion $	Y^C	3.4	WB Database
Gas Stock in Trillion $	Y^G	3.2	WB Database
Oil Stock in Trillion $	Y^O	18.6	WB Database
Cropland Stock in Trillion $	Y^L	20.8	WB Database
Minerals Stock in Trillion $	Y^M	1.2	WB Database
Forest Ecosystem Services Stock in Trillion $	Y^{FO}	7.3	WB Database
Oil Investment to Output Ratio in %	D^{FO}/Y^{FO}	0.46	Authors Calculations
Coal Investment to Output Ratio in %	D^C/Y^C	1	Authors Calculations
Gas Investment to Output Ration in %	D^G/Y^G	3.8	Authors Calculations
Renewable Investment to Output Ratio in %	D^{RE}/Y^{RE}	156.2	Authors Calculations
Minerals Investment to Output Ratio in %	D^M/Y^M	3	Authors Calculations
Land Investment to Output Ratio in %	D^L/Y^L	3	Authors Calculations
Forest Ecosystem Services Investment to Output Ratio in %	D^{FO}/Y^{FO}	3	Authors Calculations
Capital Investment to Output Ratio in %	D^K/Y^K	3	Authors Calculations

Table 27: Moments Matching

<u>Notes:</u> All the values reported in this table are perfectly matched by the model for the initial period 2018. The energy output is calculated using the electricity prices from https://www.cable.co.uk/energy/worldwide-pricing/ and quantities from Ourworldindata.

E.2 Shadow Prices Sensitivity Analysis
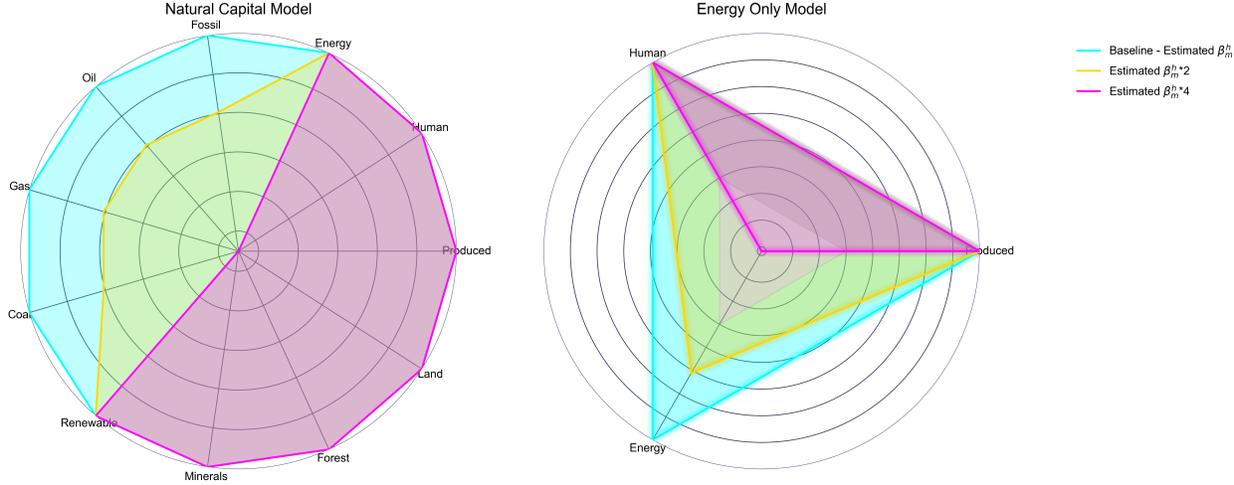
Figure 11: Shadow Prices Sensitivity To Climate Damages

Notes: This figure shows production factors' shadow prices under two different model specifications across three parameter values representing distinct scenarios. The baseline case shadow prices are normalized to one and the center of the circle correspond the lowest shadow price value.
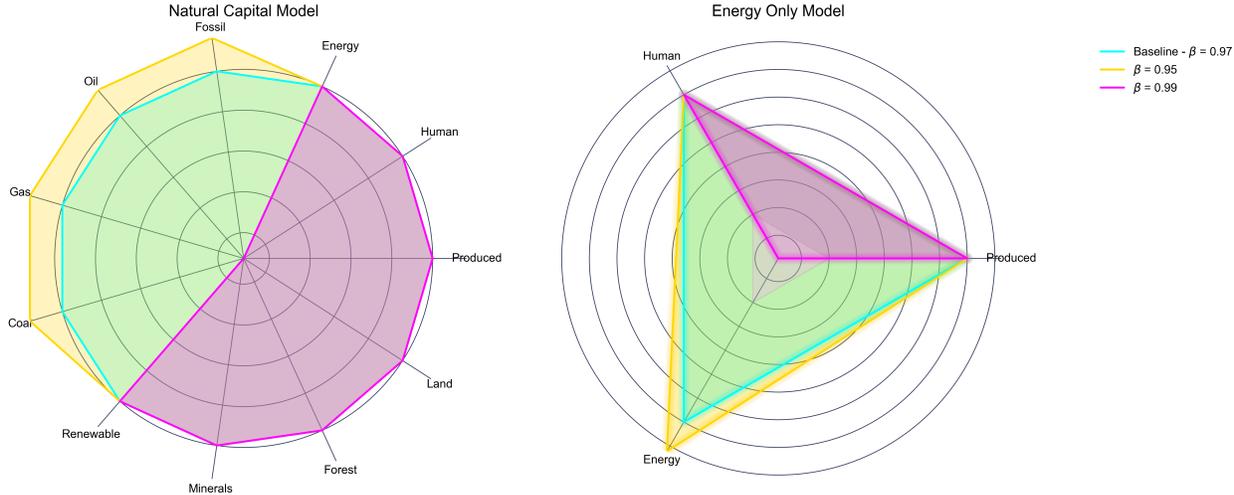
Figure 12: Natural Shadow Prices Sensitivity To Discount Rate

Notes: This figure shows production factors' shadow prices under two different model specifications across three parameter values representing distinct scenarios. The baseline case shadow prices are normalized to one and the center of the circle correspond the lowest shadow price value.
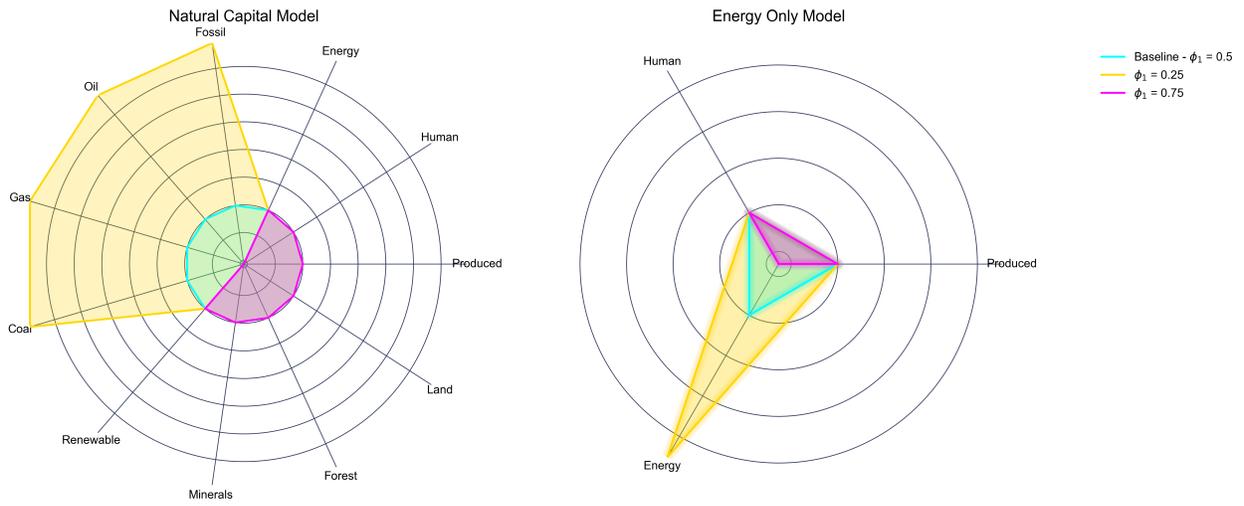
Figure 13: Natural Shadow Prices Sensitivity To Climate Sensitivity

Notes: This figure shows production factors' shadow prices under two different model specifications across three parameter values representing distinct scenarios. The baseline case shadow prices are normalized to one and the center of the circle correspond the lowest shadow price value.

E.3   Long-run Dynamics
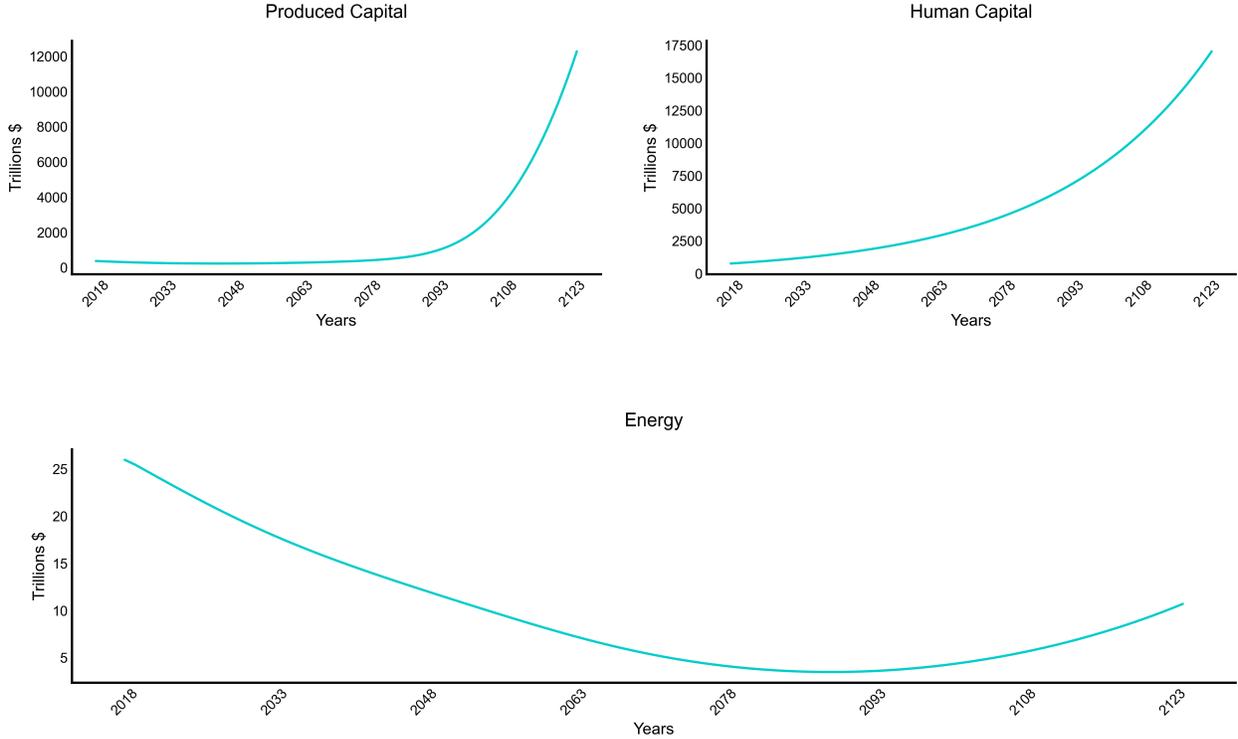
Figure 14: Long-Run Transition: Produced Capital, Human Capital, and Energy

Notes: This figure illustrates the long-run transition over 107 years (up to 2125) with a 3 percent growth rate.
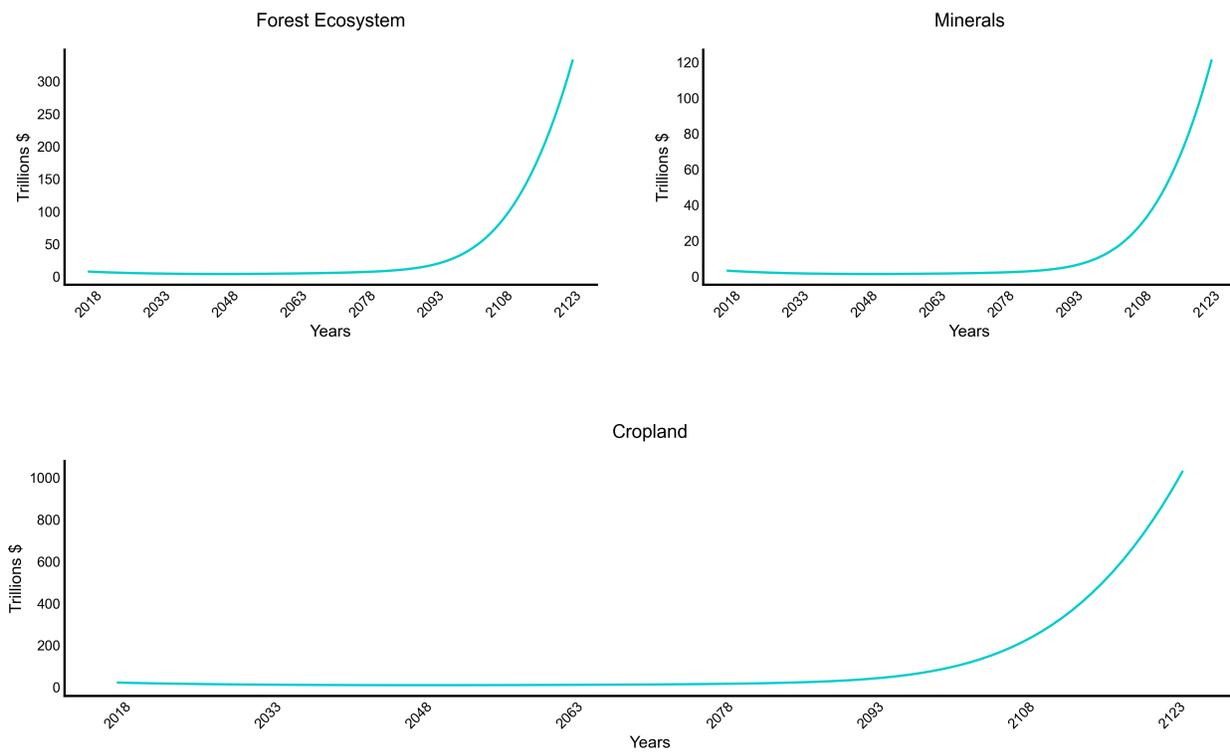
Figure 15: Long-Run Transition: Natural Capital Components

Notes: This figure illustrates the long-run transition over 107 years (up to 2125) with a 3 percent growth rate.
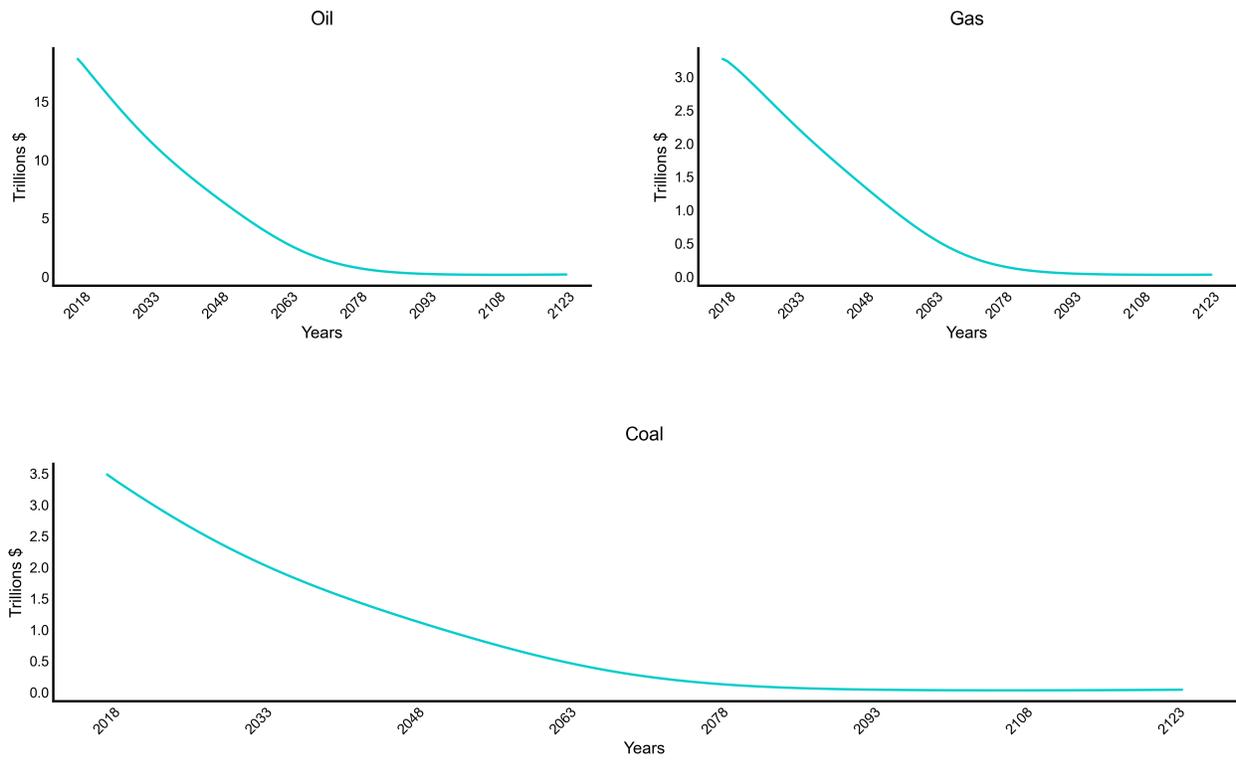
Figure 16: Long-Run Transition: Fossil Fuels Components

Notes: This figure illustrates the long-run transition over 107 years (up to 2125) with a 3 percent growth rate.

E.4   Uncertainty and Shadow Prices

Name	Variable	All Natural Capital			Only Energy		
		$\theta = 0.85$	$\theta = 0.99$	$\theta = 1.70$	$\theta = 0.85$	$\theta = 0.99$	$\theta = 1.70$
Shadow Cost of Emission	$E(V^{\mathrm{E}})$	-0.10	-0.11	-0.34	-0.09	-0.09	-0.17
		(1.18)	(1.18)	(1.20)	(1.18)	(1.18)	(1.18)
Shadow Cost of Energy	$E(\Psi^{\mathrm{E}})$	-0.01	-0.01	-0.07	0.01	0.01	0.05
		(0.12)	(0.15)	(0.38)	(0.10)	(0.13)	(0.33)
Shadow Cost of Fossil	$E(\Psi^{\mathrm{FE}})$	0.01	0.01	0.11	-	-	-
		(0.15)	(0.18)	(0.50)	-	-	-
Shadow Cost of Oil	$E(\Psi^{\mathrm{O}})$	0.01	0.01	0.11	-	-	-
		(0.15)	(0.18)	(0.50)	-	-	-
Shadow Cost of Gas	$E(\Psi^{\mathrm{G}})$	0.01	0.01	0.11	-	-	-
		(0.15)	(0.18)	(0.49)	-	-	-
Shadow Cost of Coal	$E(\Psi^{\mathrm{C}})$	0.01	0.01	0.11	-	-	-
		(0.15)	(0.18)	(0.50)	-	-	-
Shadow Cost of Renewable Energy	$E(\Psi^{\mathrm{RE}})$	0.01	0.01	0.11	-	-	-
		(0.06)	(0.06)	(0.11)	-	-	-
Shadow Cost of Minerals	$E(\Psi^{\mathrm{M}})$	0.03	0.05	0.44	-	-	-
		(0.09)	(0.11)	(0.45)	-	-	-
Shadow Cost of Eco System Services	$E(\Psi^{\mathrm{FO}})$	0.00	0.00	0.04	-	-	-
		(0.07)	(0.08)	(0.09)	-	-	-
Shadow Cost of Land	$E(\Psi^{\mathrm{L}})$	0.01	0.02	0.18	-	-	-
		(0.08)	(0.08)	(0.20)	-	-	-

Table 28: Uncertainty cost of temperature shocks for different θ values – percentage change with respect to deterministic case

Notes: This table displays the impact of temperature uncertainty on shadow prices under our two different model specifications and three cases for elasticity of substitution in the first layer. The third column corresponds to the estimated elasticity. The first column assumes an elasticity lower than unity, and the second one is an intermediate case. Results are reported as percentage deviations from the deterministic case. Standard deviations are reported in parentheses. E(X) refers to the expectation of the shadow price X.

| Name	Variable	All Natural Capital			Only Energy		
		$\theta = 0.85$	$\theta = 0.99$	$\theta = 1.70$	$\theta = 0.85$	$\theta = 0.99$	$\theta = 1.70$
Shadow Cost of Emission	$E(V^{\mathrm{E}})$	-0.10	-0.11	-0.33	-0.09	-0.09	-0.17
		(1.19)	(1.18)	(1.18)	(1.19)	(1.19)	(1.16)
Shadow Cost of Energy	$E(\Psi^{\mathrm{E}})$	-0.01	-0.01	-0.07	0.01	0.01	0.05
		(0.13)	(0.15)	(0.37)	(0.10)	(0.13)	(0.35)
Shadow Cost of Fossil	$E(\Psi^{\mathrm{FE}})$	0.01	0.01	0.11	-	-	-
		(0.18)	(0.19)	(0.51)	-	-	-
Shadow Cost of Oil	$E(\Psi^{\mathrm{O}})$	0.01	0.01	0.11	-	-	-
		(0.18)	(0.19)	(0.51)	-	-	-
Shadow Cost of Gas	$E(\Psi^{\mathrm{G}})$	0.01	0.01	0.10	-	-	-
		(0.18)	(0.19)	(0.50)	-	-	-
Shadow Cost of Coal	$E(\Psi^{\mathrm{C}})$	0.01	0.01	0.11	-	-	-
		(0.18)	(0.19)	(0.52)	-	-	-
Shadow Cost of Renewable Energy	$E(\Psi^{\mathrm{RE}})$	0.01	0.01	0.11	-	-	-
		(0.09)	(0.07)	(0.12)	-	-	-
Shadow Cost of Minerals	$E(\Psi^{\mathrm{M}})$	0.03	0.05	0.43	-	-	-
		(0.15)	(0.13)	(0.47)	-	-	-
Shadow Cost of Eco System Services	$E(\Psi^{\mathrm{FO}})$	0.00	0.00	0.04	-	-	-
		(0.12)	(0.10)	(0.15)	-	-	-
Shadow Cost of Land	$E(\Psi^{\mathrm{L}})$	0.01	0.02	0.17	-	-	-
		(0.12)	(0.10)	(0.24)	-	-	-

Table 29: Uncertainty cost of Temperature shock for different θ values – percentage change with respect to deterministic case (habits case)

Notes: This table displays the impact of temperature uncertainty on shadow prices under our two different model specifications with habit formation and three cases for elasticity of substitution in the first layer. The third column corresponds to the estimated elasticity. The first column assumes an elasticity lower than unity, and the second one is an intermediate case. Results are reported as percentage deviations from the deterministic case. Standard deviations are reported in parentheses.
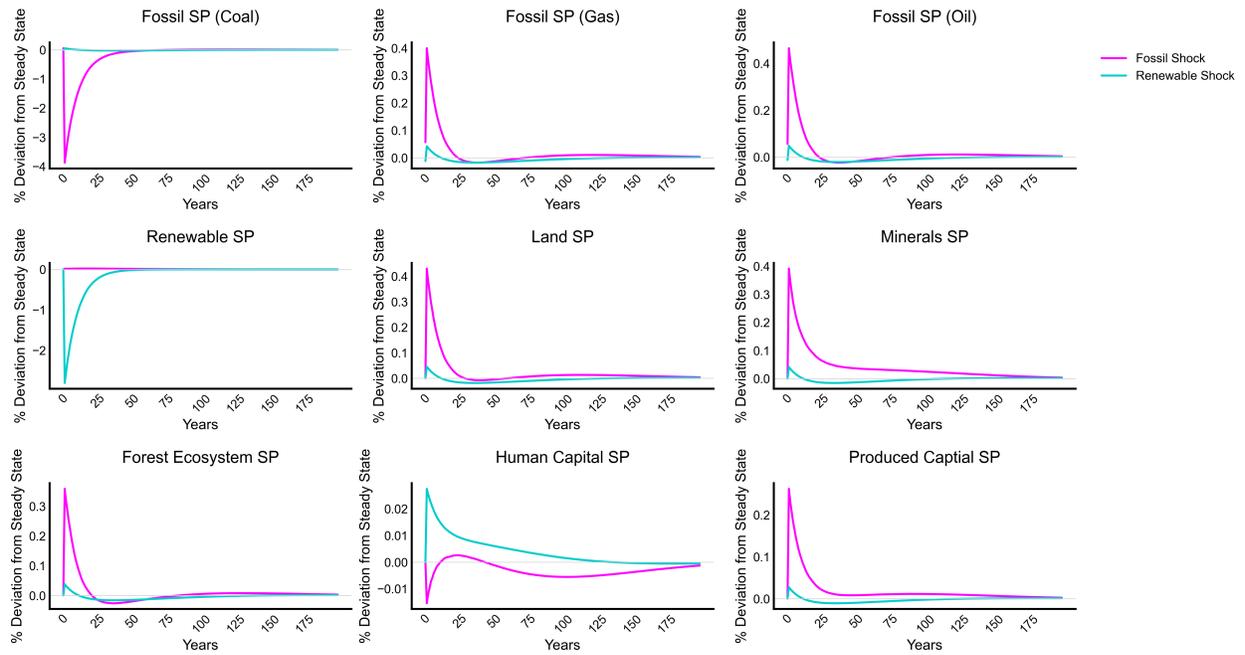
Figure 17: Impulse Response Function: Shadow Prices

Notes: This figure displays the impulse responses of the shadow prices to a shock in the intensity of coal discoveries and investment in renewables corresponding to a 5% increase in the stock of coal and renewables, respectively. The result holds for oil and gas too. The results are presented as a percentage deviation to the steady state, where the zero x-axis represents the steady state.

A CES Estimates

	Estimation Method: NLS			
	Q1	Q2	Q3	Q4
First Layer	1.4981	5.5432	2.0321	3.9432
	(0.0653)	(0.1079)	(0.0955)	(0.0471)
Second Layer	NA	NA	1.7918	2.3359
			(0.0299)	(0.0294)
Third Layer	1.2303	NA	NA	0.0116
	(0.0790)			(32.1653)

Table 30: Elasticities of Substitution by Income Quartiles (NLS)

Note: Some of the values for the elasticity of substitution are NA because the ρ parameter is -1, which is the lower bound of the estimate values. This gives infinite elasticity of substitution.

	Estimation Method: OLS			
	Q1	Q2	Q3	Q4
Second Layer	1.6844	1.7227	2.1432	1.4478
	(0.0206)	(0.0233)	(0.0291)	(0.0952)
Third Layer	NA	1.3535	NA	NA
		(0.1155)		

Table 31: Elasticities of Substitution by Income Quartiles (OLS)

Note: NA values indicate cases where the ρ parameter used to compute the elasticities is at or outside the bounds.

B Climate Damages Estimation

B.0.1 Stationarity Tests

	Statistic	p-value
Inverse chi-squared	471.278	0.000
Inverse normal	-14.789	0.000
Inverse logit	-13.906	0.000
Modified inv. chi-squared	19.285	0.000

Table 32: Panel unit-root Augmented Dickey Fueller tests results for yearly average temperature. Test statistics and p-values reported.

	Statistic	p-value
Inverse chi-squared	758.425	0.000
Inverse normal	-24.403	0.000
Inverse logit	-20.220	0.000
Modified inv. chi-squared	36.205	0.000

Table 33: Panel unit-root Augmented Dickey Fueller tests results for yearly total precipitation. Test statistics and p-values reported.

	Statistic	p-value
Inverse chi-squared	117.617	0.933
Inverse normal	0.741	0.770
Inverse logit	0.659	0.745
Modified inv. chi-squared	-1.447	0.926

Table 34: Panel unit-root Augmented Dickey Fueller tests results for coal. Test statistics and p-values reported. Model with trends.

	Statistic	p-value
Inverse chi-squared	198.550	0.001
Inverse normal	-1.353	0.088
Inverse logit	-0.908	0.182
Modified inv. chi-squared	3.356	0.000

Table 35: Panel unit-root Augmented Dickey Fueller tests results for gas. Test statistics and p-values reported. Model with trends.

	Statistic	p-value
Inverse chi-squared	277.578	0.000
Inverse normal	-5.132	0.000
Inverse logit	-4.556	0.000
Modified inv. chi-squared	7.871	0.000

Table 36: Panel unit-root Augmented Dickey Fueller tests results for oil. Test statistics and p-values reported. Model with trends.

	Statistic	p-value
Inverse chi-squared	185.915	0.011
Inverse normal	-1.235	0.109
Inverse logit	-1.129	0.130
Modified inv. chi-squared	2.470	0.007

Table 37: Panel unit-root Augmented Dickey Fueller tests results for fossil fuel. Test statistics and p-values reported. Model with trends.

	Statistic	p-value
Inverse chi-squared	163.741	0.124
Inverse normal	-0.798	0.213
Inverse logit	-0.604	0.273
Modified inv. chi-squared	1.163	0.122

Table 38: Panel unit-root Augmented Dickey Fueller tests results for gas aggregate energy. Test statistics and p-values reported. Model with trends.

	Statistic	p-value
Inverse chi-squared	186.098	0.010
Inverse normal	-0.264	0.396
Inverse logit	-0.018	0.493
Modified inv. chi-squared	2.481	0.007

Table 39: Panel unit-root Augmented Dickey Fueller tests results for renewable electricity. Test statistics and p-values reported. Model with trends.

	Statistic	p-value
Inverse chi-squared	182.514	0.016
Inverse normal	-0.861	0.195
Inverse logit	-0.615	0.269
Modified inv. chi-squared	2.269	0.012

Table 40: Panel unit-root Augmented Dickey Fueller tests results for forest ecosystem. Test statistics and p-values reported. Model with trends.

	Statistic	p-value
Inverse chi-squared	169.586	0.071
Inverse normal	-3.196	0.001
Inverse logit	-2.225	0.013
Modified inv. chi-squared	1.508	0.066

Table 41: Panel unit-root Augmented Dickey Fueller tests results for minerals. Test statistics and p-values reported.

	Statistic	p-value
Inverse chi-squared	262.336	0.000
Inverse normal	-1.380	0.084
Inverse logit	0.793	0.786
Modified inv. chi-squared	6.973	0.000

Table 42: Panel unit-root Augmented Dickey Fueller tests results for cropland. Test statistics and p-values reported.

C Non-Detrended Economy

C.1 Social Planner Equilibrium: Complete Model

Consistent with the model section, the following notations are used:

$i \in \{Y_t^O, Y_t^G, Y_t^C\}$

$j \in \{Y_t^K, Y_t^M, Y_t^L, Y_t^{FO}\}$

$k \in \{Y_t^K, Y_t^{AL}, Y_t^E, Y_t^L, Y_t^M, Y_t^{FO}\}$

$h \in \{i\} \cup \{j\} \cup \{RE\}$

The social planner face the following maximization problem:

$$
\begin{aligned}
\mathcal{L} = E_0 \sum_{t=0}^{\infty} \beta^t \Bigg\{ & \frac{(C_t - \gamma_H H_t)^{1-\sigma^H}}{1-\sigma} \\
& + \lambda_t^C \left[Y_t^T - C_t - \sum_h D_t^h \right] \\
& + \lambda_t^C \lambda_t^H \left[H_{t+1} - m H_t - (1-m) C_t \right] \\
& + \lambda_t^C V_t^T \left[T_{t+1} - T_t - \epsilon_t^T \phi_1 \left(\phi_2 X_t - T_t \right) \right] \\
& + \lambda_t^C V_t^X \left[X_{t+1} - X_t - E_t \right] \\
& + \lambda_t^C V_t^E \left[E_t - \phi_E Y_t^{FE} \right] \\
& + \lambda_t^C \Psi_t^{AL} \left[e^{d_{AL}(\cdot)} A_t L_t - Y_t^{AL} \right] \\
& + \sum_h \lambda_t^C \Psi_t^h \left[e^{d_h(\cdot)} S_t^h - Y_t^h \right] \\
& + \sum_h \lambda_t^C \mathcal{R}_t^h \left[S_t^h + \epsilon_t^{D_h} \alpha_h D_t^h - \delta_h S_t^h - S_{t+1}^h \right] \\
& + \lambda_t^C \Psi_t^{FE} \left[g_{FE} \left(\sum_i \epsilon_i (Y_t^i)^{\frac{\epsilon-1}{\epsilon}} \right)^{\frac{\epsilon}{1-\epsilon}} - Y_t^{FE} \right] \\
& + \lambda_t^C \Psi_t^E \left[g_E \left(\sigma_{FE} (Y_t^{FE})^{\frac{\sigma-1}{\sigma}} + \sigma_{RE} (Y_t^{RE})^{\frac{\sigma-1}{\sigma}} \right)^{\frac{\sigma}{1-\sigma}} - Y_t^E \right] \\
& + \lambda_t^C \Psi_t^T \left[\epsilon_t^A g_Y \left(\sum_k \gamma_k (Y_t^k)^{\frac{\theta-1}{\theta}} \right)^{\frac{\theta}{1-\theta}} - Y_t^T \right] \Bigg\}
\end{aligned}
$$

This yields the first order conditions (FOCs) with respect to:

$$K_{t+1}, H_{t+1}, X_{t+1}, T_{t+1}, C_t, E_t, Y_t^{\mathrm{AL}}, Y_t^h, Y_t^{\mathrm{FE}}, Y_t^{\mathrm{RE}}, Y_t^{\mathrm{E}}, Y_t^T, S_{t+1}^h, D_t^h$$

The FOCs read as:

$$[C_t] : (C_t - \gamma_H H_t)^{-\sigma^H} = \lambda_t^C + \lambda_t^C \lambda_t^H (1 - m)$$

$$[H_{t+1}] : \lambda_t^C \lambda_t^H = \beta E_t \left\{ \gamma_H (C_{t+1} - H_{t+1})^{-\sigma} + m \lambda_{t+1}^C \lambda_{t+1}^H \right\}$$

$$[X_{t+1}] : \lambda_t^C V_t^X = \beta E_t \left\{ \lambda_{t+1}^C \left[V_{t+1}^X + \epsilon_{t+1}^T \phi_1 \phi_2 V_{t+1}^T \right] \right\}$$

$$[T_{t+1}] : V_t^T = \beta E_t \left\{ \frac{\lambda_{t+1}^C}{\lambda_t^C} \left[(1 - \epsilon_{t+1}^T \phi_1) \right] V_{t+1}^T \right\} - \sum_h \sum_m E_{t+m} \left\{ \left[\left(\prod_{o=0}^{m-1} \beta \frac{\lambda_{t+1+o}^C}{\lambda_{t+o}^C} \right) \Psi_{t+m}^h \beta_m^h Y_{t+m}^h \right] \right\}$$

$$[E_t] : V_t^X = V_t^E$$

$$[S_{t+1}^h] : \mathcal{R}_t^h = E_t \left\{ \beta \frac{\lambda_{+1}^C}{\lambda_t^C} \left[(1 - \delta_h) \mathcal{R}_{t+1}^h + e^{d_h(T_{t+1})} \Psi_{t+1}^h \right] \right\}$$

$$[D_t^h] : \mathcal{R}_t^h = \frac{1}{\epsilon_t^{D_h} \alpha_h}$$

$$[Y_t^{\mathrm{AL}}] : \Psi_t^{\mathrm{AL}} = \Psi_t^T \gamma_{\mathrm{AL}} \left(Y_t^{\mathrm{AL}} \right)^{-\frac{1}{\theta}} \left(Y_t^T \right)^{\frac{1}{\theta}} \left(\epsilon_t^A g_Y \right)^{\frac{\theta-1}{\theta}}$$

$$[Y_t^i] : \Psi_t^i = \Psi_t^{\mathrm{FE}} \epsilon_i \left(Y_t^i \right)^{-\frac{1}{\epsilon}} \left(Y_t^{\mathrm{FE}} \right)^{\frac{1}{\epsilon}} g_{\mathrm{FE}}^{\frac{\epsilon-1}{\epsilon}}$$

$$\left[Y_t^j \right] : \Psi_t^j = Y_t^T \gamma_j \left(Y_t^j \right)^{-\frac{1}{\theta}} \left(Y_t^T \right)^{\frac{1}{\theta}} \left(\epsilon_t^A g_Y \right)^{\frac{\theta-1}{\theta}}$$

$$[Y_t^{\mathrm{FE}}] : \Psi_t^{\mathrm{FE}} = \Psi_t^{\mathrm{E}} \sigma_{\mathrm{FE}} \left(Y_t^{\mathrm{FE}} \right)^{-\frac{1}{\sigma}} \left(Y_t^{\mathrm{E}} \right)^{\frac{1}{\sigma}} g_E^{\frac{\sigma-1}{\sigma}} - \phi_E V_t^E$$

$$[Y_t^{\mathrm{RE}}] : \Psi_t^{\mathrm{RE}} = \Psi_t^{\mathrm{E}} \sigma_{\mathrm{RE}} \left(Y_t^{\mathrm{RE}} \right)^{-\frac{1}{\sigma}} \left(Y_t^{\mathrm{E}} \right)^{\frac{1}{\sigma}} g_E^{\frac{\sigma-1}{\sigma}}$$

$$[Y_t^{\mathrm{E}}] : \Psi_t^{\mathrm{E}} = \Psi_t^{\mathrm{T}} \sigma_{\mathrm{E}} \left(Y_t^{\mathrm{E}} \right)^{-\frac{1}{\theta}} \left(Y_t^T \right)^{\frac{1}{\theta}} \left(\epsilon_t^A g_Y \right)^{\frac{\theta-1}{\theta}}$$

$$\left[Y_t^{\mathrm{T}} \right] : \Psi_t^T = 1$$

C.2 Social Planner Equilibrium: Model with Fossil Energy Only

The social planner problem for the reduced form model with fossil fuel energy only reads as:

$$
\begin{aligned}
\mathcal{L} = E_0 \sum_{t=0}^{\infty} \beta^t \Bigg\{ & \frac{(C_t - \gamma_H H_t)^{1-\sigma}}{1 - \sigma^H} \\
& + \lambda_t^C \left[Y_t^T - C_t - D_t^K - D_t^{FE} \right] \\
& + \lambda_t^C \lambda_t^H \left[H_{t+1} - m H_t - (1-m) C_t \right] \\
& + \lambda_t^C V_t^T \left[T_{t+1} - T_t - \epsilon_t^T \phi_1 \left(\phi_2 X_t - T_t \right) \right] \\
& + \lambda_t^C V_t^X \left[X_{t+1} - X_t - E_t \right] \\
& + \lambda_t^C V_t^E \left[E_t - \phi_E Y_t^{FE} \right] \\
& + \lambda_t^C \Psi_t^{AL} \left[e^{d_{AL}(\cdot)} A_t L_t - Y_t^{AL} \right] \\
& + \lambda_t^C \Psi_t^{K} \left[e^{d_K(\cdot)} S_t^{K} - Y_t^{K} \right] \\
& + \lambda_t^C \Psi_t^{FE} \left[e^{d_{FE}(\cdot)} S_t^{FE} - Y_t^{FE} \right] \\
& + \lambda_t^C \mathcal{R}_t^{K} \left[S_t^{K} + \epsilon_t^{D_K} \alpha_K D_t^{K} - \delta_K S_t^{K} - S_{t+1}^{K} \right] \\
& + \lambda_t^C \mathcal{R}_t^{FE} \left[S_t^{FE} + \epsilon_t^{D_{FE}} \alpha_{FE} D_t^{FE} - \delta_{FE} S_t^{FE} - S_{t+1}^{FE} \right] \\
& + \lambda_t^C \Psi_t^{T} \left[\epsilon_t^A g_Y \left(\gamma_K \left(Y_t^K \right)^{\frac{\theta-1}{\theta}} + \gamma_{FE} \left(Y_t^{FE} \right)^{\frac{\theta-1}{\theta}} + \gamma_{AL} \left(Y_t^{AL} \right)^{\frac{\theta-1}{\theta}} \right)^{\frac{\theta}{1-\theta}} - Y_t^{T} \right] \Bigg\}
\end{aligned}
$$

In the following, we present all first-order conditions (FOCs). Notice that the FOCs with respect to: $T_{t+1}, Y_t^T, Y_t^{FE}, S_{t+1}^{FE}, D_t^{FE}$ differ from those in the full model case, while the remaining FOCs (with respect to $H_{t+1}, X_{t+1}, C_t, E_t, Y_t^{AL}, Y_t^{K}, S_{t+1}^{K}, D_t^{K}$) remain similar to those in the full-scale model with all natural capital.

The FOCs read as:

$$[C_t] : (C_t - \gamma_H H_t)^{-\sigma} = \lambda_t^C + \lambda_t^C \lambda_t^H (1 - m)$$

$$[H_{t+1}] : \lambda_t^C \lambda_t^H = \beta E_t \left\{ \gamma_H (C_{t+1} - H_{t+1})^{-\sigma} + m \lambda_{t+1}^C \lambda_{t+1}^H \right\}$$

$$[X_{t+1}] : \lambda_t^C V_t^X = \beta E_t \left\{ \lambda_{t+1}^C \left[V_{t+1}^X + \epsilon_{t+1}^T \phi_1 \phi_2 V_{t+1}^T \right] \right\}$$

$$[T_{t+1}] : V_t^T = \beta E_t \left\{ \frac{\lambda_{t+1}^C}{\lambda_t^C} \left[(1 - \epsilon_{t+1}^T \phi_1) \right] V_{t+1}^T \right\} - \sum_h \sum_m E_{t+m} \left\{ \left[\left(\prod_{o=0}^{m-1} \beta \frac{\lambda_{t+1+o}^C}{\lambda_{t+o}^C} \right) \Psi_{t+m}^h \beta_m^h Y_{t+m}^h \right] \right\}$$

$$[E_t] : V_t^X = V_t^E$$

$$[S_{t+1}^{\mathrm{K}}] : \mathcal{R}_t^{\mathrm{K}} = E_t \left\{ \beta \frac{\lambda_{+1}^C}{\lambda_t^C} \left[(1 - \delta_{\mathrm{K}}) \mathcal{R}_{t+1}^{\mathrm{K}} + e^{d_{\mathrm{K}}(T_{t+1})} \Psi_{t+1}^{\mathrm{K}} \right] \right\}$$

$$[S_{t+1}^{\mathrm{FE}}] : \mathcal{R}_t^{\mathrm{FE}} = E_t \left\{ \beta \frac{\lambda_{+1}^C}{\lambda_t^C} \left[(1 - \delta_{\mathrm{FE}}) \mathcal{R}_{t+1}^{\mathrm{FE}} + e^{d_{\mathrm{FE}}(T_{t+1})} \Psi_{t+1}^{\mathrm{FE}} \right] \right\}$$

$$[D_t^{\mathrm{K}}] : \mathcal{R}_t^{\mathrm{K}} = \frac{1}{\epsilon_t^{D_K} \alpha_{\mathrm{K}}}$$

$$[D_t^{\mathrm{FE}}] : \mathcal{R}_t^{\mathrm{FE}} = \frac{1}{\epsilon_t^{D_F E} \alpha_{\mathrm{FE}}}$$

$$[Y_t^{\mathrm{AL}}] : \Psi_t^{\mathrm{AL}} = \Psi_t^T \gamma_{\mathrm{AL}} \left(Y_t^{\mathrm{AL}} \right)^{-\frac{1}{\theta}} \left(Y_t^T \right)^{\frac{1}{\theta}} \left(\epsilon_t^A g_Y \right)^{\frac{\theta-1}{\theta}}$$

$$[Y_t^{\mathrm{FE}}] : \Psi_t^{\mathrm{FE}} = \Psi_t^T \gamma_{\mathrm{FE}} \left(Y_t^{\mathrm{FE}} \right)^{-\frac{1}{\theta}} \left(Y_t^T \right)^{\frac{1}{\theta}} \left(\epsilon_t^A g_Y \right)^{\frac{\theta-1}{\theta}} - \phi_E V_t^E$$

$$[Y_t^{\mathrm{T}}] : \Psi_t^T = 1$$

where h here is produced capital, fossil energy, and labour production.

D   Stationary Equilibrium

D.1   The Balanced Growth Path: (For Both Models)

In this section, we present the detrended model around its balanced growth path (BGP). We denote all stationary variables with lower case letters (e.g. x_t), while variables following the trend will be referred with capital letters (e.g. X_t).

Consistent with the model section, the following notations are used:

$i \in \left\{ Y_t^O, Y_t^G, Y_t^C \right\}$

$j \in \left\{ Y_t^M, Y_t^L, Y_t^{FO} \right\}$

$k \in \left\{ Y_t^K, Y_t^E, Y_t^L, Y_t^M, Y_t^{FO} \right\}$

$h \in \{i\} \cup \{j\} \cup \{RE\}$

Labor-augmenting technological change is subject to an exogenous growth process Γ_t such that $\Gamma_t = \gamma^\Gamma \Gamma_{t-1}$ and where:

$$Y_t^{AL} = e^{d(\cdot)} A(\Gamma_t \bar{L}) \tag{32}$$

where both A and L are stationary variables. Thus,

$$y_t^{AL} = e^{d(\cdot)} A\bar{L} \tag{33}$$

and where $y_t^{AL} = \frac{Y_t^{AL}}{\Gamma_t}$ Similarly, aggregate output reads as:

$$Y_t^T = \epsilon_t^A g_Y \left(\sum_k \gamma_k \left(Y_t^k \right)^{\frac{\theta-1}{\theta}} + \gamma_{AL} \left(Y_t^{AL} \right)^{\frac{\theta-1}{\theta}} \right)^{\frac{\theta}{1-\theta}} \tag{34}$$

The detrended output reads as:

$$y_t^T = \epsilon_t^A g_Y \left(\sum_k \gamma_k \left(y_t^k \right)^{\frac{\theta-1}{\theta}} + \gamma_{AL} \left(y_t^{AL} \right)^{\frac{\theta-1}{\theta}} \right)^{\frac{\theta}{1-\theta}} \tag{35}$$

where $y_t^T = \frac{Y_t^T}{\Gamma_t}$ and $y_t^k = \frac{Y_t^k}{\Gamma_t}$

As such all capitals in the economy grow at rate γ^Γ with:

$$\gamma^\Gamma s_{t+1}^h = \epsilon_t^{D_h} \alpha_h d_t^h + (1 - \delta_h) s_t^h \tag{36}$$

where $d_t^h = \frac{D_t^h}{\Gamma_t}$ and $s_t^h = \frac{S_t^h}{\Gamma_t}$.

Since fossil energy grows at rate γ^Γ, so do CO_2 emissions:

$$e_t = \phi_E y_t^F \tag{37}$$

with $e_t = \frac{E_t}{\Gamma_t}$.

Cumulative emissions and temperature will also follow the same economy growth rate:

$$\gamma^\Gamma x_{t+1} = x_t + e_t \tag{38}$$

$$\gamma^\Gamma t_{t+1} = \epsilon_t^T \phi_1 (\phi_2 x_t - t_t) + t_t \tag{39}$$

The damage functions are stationary with $\tilde{\beta}_m^h = \beta_m^h \Gamma_{t-m}$:[32]

$$d(\cdot) = \sum_m \tilde{\beta}_m^h t_{t-m} \tag{40}$$

Finally the detrended utility function reads as:

$$E_0 \sum_{t=0}^\infty \tilde{\beta}^t \left\{ \frac{(c_t - \gamma_H h_t)^{1-\sigma^H}}{1 - \sigma} \right\} \tag{41}$$

where $\tilde{\beta}^t = \beta^t \Gamma_t^{1-\sigma}$.

In the case of the model with fossil fuel only, please notice that all variables are detrended similarly to the full model. Essentially, the model with fossil fuel only is a special case of the large model with different natural capitals.

D.2   The Social Planner

The social planner face the same maximization problem presented above:

---

[32]An assumption we will make when focusing on the long-run transitions is: $\tilde{\beta}_m^h \approx \beta_m^h$ in order to make sure damages are not decreasing overtime.

$$\mathcal{L} = E_0 \sum_{t=0}^{\infty} \tilde{\beta}^t \left\{ \frac{(c_t - \gamma_H h_t)^{1-\sigma^H}}{1-\sigma} \right.$$

$$+ \lambda_t^C \left[y_t^T - c_t - \sum_h d_t^h \right]$$

$$+ \lambda_t^C \lambda_t^H \left[\gamma^\Gamma h_{t+1} - m h_t - (1-m)c_t \right]$$

$$+ \lambda_t^C v_t^T \left[\gamma^\Gamma t_{t+1} - t_t - \epsilon_t^T \phi_1 \left(\phi_2 x_t - t_t \right) \right]$$

$$+ \lambda_t^C v_t^X \left[\gamma^\Gamma x_{t+1} - x_t - e_t \right]$$

$$+ \lambda_t^C v_t^E \left[e_t - \phi_E y_t^{\mathrm{FE}} \right]$$

$$+ \lambda_t^C \psi_t^{\mathrm{AL}} \left[e^{d_{\mathrm{AL}}(\cdot)} A_t L_t - y_t^{\mathrm{AL}} \right]$$

$$+ \sum_h \lambda_t^C \psi_t^h \left[e^{d_h(\cdot)} s_t^h - y_t^h \right]$$

$$+ \sum_h \lambda_t^C r_t^h \left[s_t^h + \epsilon_t^{D_h} \alpha_h d_t^h - \delta_h s_t^h - \gamma^\Gamma s_{t+1}^h \right]$$

$$+ \lambda_t^C \psi_t^{\mathrm{FE}} \left[g_{\mathrm{FE}} \left(\sum_i \epsilon_i \left(y_t^i \right)^{\frac{\epsilon-1}{\epsilon}} \right)^{\frac{\epsilon}{1-\epsilon}} - y_t^{\mathrm{FE}} \right]$$

$$+ \lambda_t^C \psi_t^E \left[g_E \left(\sigma_{\mathrm{FE}} \left(y_t^{\mathrm{FE}} \right)^{\frac{\sigma-1}{\sigma}} + \sigma_{\mathrm{RE}} \left(y_t^{\mathrm{RE}} \right)^{\frac{\sigma-1}{\sigma}} \right)^{\frac{\sigma}{1-\sigma}} - y_t^E \right]$$

$$+ \lambda_t^C \psi_t^T \left[\epsilon_t^A g_Y \left(\sum_k \gamma_k \left(y_t^k \right)^{\frac{\theta-1}{\theta}} \right)^{\frac{\theta}{1-\theta}} - y_t^T \right] \right\}$$

This yields the first order conditions (FOCs) with respect to:

$$k_{t+1}, h_{t+1}, x_{t+1}, t_{t+1}, c_t, e_t, y_t^{\mathrm{AL}}, y_t^h, y_t^{\mathrm{FE}}, y_t^{\mathrm{RE}}, y_t^E, y_t^T, s_{t+1}^h, d_t^h$$

The FOCs read as:

$$[c_t] : (c_t - \gamma_H h_t)^{-\sigma^H} = \lambda_t^C + \lambda_t^C \lambda_t^H (1-m)$$

$$[h_{t+1}] : \gamma^\Gamma \lambda_t^C \lambda_t^H = \tilde{\beta} E_t \left\{ \gamma_H (c_{t+1} - h_{t+1})^{-\sigma} + m \lambda_{t+1}^C \lambda_{t+1}^H \right\}$$

$$[x_{t+1}] : \gamma^\Gamma \lambda_t^C v_t^X = \tilde{\beta} E_t \left\{ \lambda_{t+1}^C \left[v_{t+1}^X + \epsilon_{t+1}^T \phi_1 \phi_2 v_{t+1}^T \right] \right\}$$

$$[t_{t+1}] : \gamma^\Gamma v_t^T = \tilde{\beta} E_t \left\{ \frac{\lambda_{t+1}^C}{\lambda_t^C} \left[(1 - \epsilon_{t+1}^T \phi_1) \right] v_{t+1}^T \right\} - \sum_h \sum_m E_{t+m} \left\{ \left[\left(\prod_{o=0}^{m-1} \tilde{\beta} \frac{\lambda_{t+1+o}^C}{\lambda_{t+o}^C} \right) \psi_{t+m}^h \tilde{\beta}_m^h y_{t+m}^h \right] \right\}$$

$$[e_t] : v_t^X = v_t^E$$

$$[s_{t+1}^h] : \gamma^\Gamma r_t^h = E_t \left\{ \tilde{\beta} \frac{\lambda_{+1}^C}{\lambda_t^C} \left[(1 - \delta_h) r_{t+1}^h + e^{d_h(T_{t+1})} \psi_{t+1}^h \right] \right\}$$

$$[d_t^h] : r_t^h = \frac{1}{\epsilon_t^{D_h} \alpha_h}$$

$$[y_t^{\text{AL}}] : \psi_t^{\text{AL}} = \psi_t^T \gamma_{\text{AL}} \left(y_t^{\text{AL}} \right)^{-\frac{1}{\theta}} \left(y_t^T \right)^{\frac{1}{\theta}} \left(\epsilon_t^A g_Y \right)^{\frac{\theta-1}{\theta}}$$

$$[y_t^i] : \psi_t^i = \psi_t^{\text{FE}} \epsilon_i \left(y_t^i \right)^{-\frac{1}{\epsilon}} \left(y_t^{\text{FE}} \right)^{\frac{1}{\epsilon}} g_{\text{FE}}^{\frac{\epsilon-1}{\epsilon}}$$

$$[y_t^j] : \psi_t^j = y_t^T \gamma_j \left(y_t^j \right)^{-\frac{1}{\theta}} \left(y_t^T \right)^{\frac{1}{\theta}} \left(\epsilon_t^A g_Y \right)^{\frac{\theta-1}{\theta}}$$

$$[y_t^{\text{FE}}] : \psi_t^{\text{FE}} = \psi_t^E \sigma_{\text{FE}} \left(y_t^{\text{FE}} \right)^{-\frac{1}{\sigma}} \left(y_t^E \right)^{\frac{1}{\sigma}} g_E^{\frac{\sigma-1}{\sigma}} - \phi_E v_t^E$$

$$[y_t^{\text{RE}}] : \psi_t^{\text{RE}} = \psi_t^E \sigma_{\text{RE}} \left(y_t^{\text{RE}} \right)^{-\frac{1}{\sigma}} \left(y_t^E \right)^{\frac{1}{\sigma}} g_E^{\frac{\sigma-1}{\sigma}}$$

$$[y_t^E] : \psi_t^E = \psi_t^T \sigma_E \left(y_t^E \right)^{-\frac{1}{\theta}} \left(y_t^T \right)^{\frac{1}{\theta}} \left(\epsilon_t^A g_Y \right)^{\frac{\theta-1}{\theta}}$$

$$[y_t^T] : \psi_t^T = 1$$

Notice that the fossil energy only model's detrended equilibrium FOC(s) remain similar to the non-detrended case and will be adjusted similar to what we presented in the case of the full detrended model presented just above.